Significant Findings: Tracking the SeaWiFS Record with a Coupled Physical/Biogeochemical/Radiative Model of the Global Oceans

Watson W. Gregg

Submitted to Deep Sea Research 2000

The Sea-Viewing Wide Field-of-view Sensor (SeaWiFS) has observed 2.5 years of routine global chlorophyll observations from space. The mission was launched into a record El Niño event, which eventually gave way to one of the most intensive and longest-lasting La Niña events ever recorded. The SeaWiFS chlorophyll record captured the response of ocean phytoplankton to these significant events in the tropical Indo-Pacific basins, but also indicated significant interannual variability unrelated to the El Niño/La Niña events. This included large variability in the North Atlantic and Pacific basins, in the North Central and equatorial Atlantic, and milder patterns in the North Central Pacific.

This SeaWiFS record was tracked with a coupled physical/biogeochemical/radiative model of the global oceans using near-real-time forcing data such as wind stresses, sea surface temperatures, and sea ice. This provided an opportunity to offer physically and biogeochemically meaningful explanations of the variability observed in the SeaWiFS data set, since the causal mechanisms and interrelationships of the model are completely understood.

The coupled model was able to represent the seasonal distributions of chlorophyll during the SeaWiFS era, and was capable of differentiating among the widely different processes and dynamics occurring in the global oceans. The model was also reasonably successful in representing the interannual signal, especially when it was large, such as the El Niño and La Niña events in the tropical Pacific and Indian Oceans. The model provided different phytoplankton group responses for the different events in these regions: diatoms were predominant in the tropical Pacific during the La Niña but other groups were predominant during El Niño. The opposite condition occurred in the tropical Indian Ocean. Both situations were due to the different responses of the basins to El Niño. The interannual variability in the North Atlantic, which was exhibited in SeaWiFS data as a decline in the spring/summer bloom in 1999 relative to 1998, resulted in the model from a more slowly shoaling mixed layer, allowing herbivore populations to keep pace with increasing phytoplankton populations. However, several aspects of the interannual cycle were not well-represented by the model. Explanations ranged from inherent model deficiencies, to monthly averaging of forcing fields, to biases in SeaWiFS atmospheric correction procedures.

Science Priorities: Tracking the SeaWiFS Record with a Coupled Physical/Biogeochemical/Radiative Model of the Global Oceans

Watson W. Gregg

Submitted to Deep Sea Research 2000

Priority#1 Land Cover Change and Global Productivity

Tracking the SeaWiFS Record with a Coupled Physical/Biogeochemical/Radiative Model of the Global Oceans

Watson W. Gregg

NASA/Goddard Space Flight Center, Laboratory for Hydrospheric Processes, Greenbelt, MD 20771. gregg@cabin.gsfc.nasa.gov

Abstract

The Sea-Viewing Wide Field-of-view Sensor (SeaWiFS) has observed 2.5 years of routine global chlorophyll observations from space. The mission was launched into a record El Niño event, which eventually gave way to one of the most intensive and longest-lasting La Niña events ever recorded. The SeaWiFS chlorophyll record captured the response of ocean phytoplankton to these significant events in the tropical Indo-Pacific basins, but also indicated significant interannual variability unrelated to the El Niño/La Niña events. This included large variability in the North Atlantic and Pacific basins, in the North Central and equatorial Atlantic, and milder patterns in the North Central Pacific.

This SeaWiFS record was tracked with a coupled physical/biogeochemical/radiative model of the global oceans using near-real-time forcing data such as wind stresses, sea surface temperatures, and sea ice. This provided an opportunity to offer physically and biogeochemically meaningful explanations of the variability observed in the SeaWiFS data set, since the causal mechanisms and interrelationships of the model are completely understood.

The coupled model was able to represent the seasonal distributions of chlorophyll during the SeaWiFS era, and was capable of differentiating among the widely different processes and dynamics occurring in the global oceans. The model was also reasonably successful in representing the interannual signal, especially when it was large, such as the El Niño and La Niña events in the tropical Pacific and Indian Oceans. The model provided different phytoplankton group responses for the different events in these regions: diatoms were predominant in the tropical Pacific during the La Niña but other groups were predominant during El Niño. The opposite condition occurred in the tropical Indian Ocean. Both situations were due to the different responses of the basins to El Niño. The interannual variability in the North Atlantic, which was exhibited in SeaWiFS data as a decline in the spring/summer bloom in 1999 relative to 1998, resulted in the model from a more slowly shoaling mixed layer, allowing herbivore populations to keep pace with increasing phytoplankton populations. However, several aspects of the interannual cycle were not well-represented by the model. Explanations ranged from inherent model deficiencies, to monthly averaging of forcing fields, to biases in SeaWiFS atmospheric correction procedures.

1. Introduction

The Sea-Viewing Wide Field-of-view Sensor (SeaWiFS; McClain et al., 1998) is into its third year collecting routine global chlorophyll observations from space. This represents an unprecedented data set in terms of coverage, continuity, and duration that enables us for the first time to make meaningful observations about the state of biological components in the global oceans, their spatial variability, and their medium-term (interannual) variability. This

latter point especially differentiates SeaWiFS from the two previous large-scale-coverage missions, the Coastal Zone Color Scanner (CZCS), which did not provide routine global coverage in its 8-year lifetime (Feldman et al., 1989), and the Ocean Color and Temperature Scanner (OCTS), which failed after nine months of on-orbit operations (Shimoda, 1999).

The comprehensive SeaWiFS data set, lasting from September 1997 to the present, provides an opportunity to observe the behavior of ocean phytoplankton in response to medium-term natural variability, i.e., seasonal and interannual variability. If analysis of this record is combined with the outputs of a coupled physical/biogeochemical model whose dynamical features are completely understood, then insights may be gained into the causes of this variability, especially when the results are in agreement. Even when they are not, this combination of analysis methodologies can help us infer what processes are not incorporated into the model and their apparent importance.

Such application of coupled three-dimensional physical/biological models on basin (e.g., Dutkiewicz et al., 2000; McGillicuddy et al., 1995; Sarmiento et al., 1993) and regional scales (e.g., Walsh et al., 1999; Gregg and Walsh, 1992) has achieved considerable success relating outputs to in situ and satellite observations. In this paper we adapt an existing coupled physical/biogeochemical/radiative model of the global oceans (Gregg, 2000) to the atmospheric and oceanic forcing conditions present during the SeaWiFS era (Sep. 1997 to Feb. 2000) and track the results as compared to SeaWiFS chlorophyll data on synoptic and basin scales. The fact that SeaWiFS in its short lifetime has experienced significant anomalous conditions (El Niño and La Niña) provides an enhanced opportunity to evaluate the nature of the dynamical processes involved and the interactions of biological processes with physical ones.

2. Materials and Methods

2.1 SeaWiFS Data

A global comparison of SeaWiFS chlorophyll data, provided by the NASA/Goddard Space Flight Center (GSFC)/Distributed Active Archive Center (DAAC) with the CZCS archive, the entire in-situ data archive maintained by NOAA/National Oceanographic Data Center (NODC), and a blended analysis using in-situ data and the CZCS archive (Gregg and Conkright, 2000), suggested that SeaWiFS data tended to overestimate chlorophyll concentrations (Conkright and Gregg, 2000). This was attributed to 1) errors associated with the assumption that water-leaving radiances at the near-infrared (NIR) bands of SeaWiFS are negligible, and 2) bio-optical algorithm. An excessively large number of maximum chlorophyll concentrations (64 mg m^{-3}) were produced by the SeaWiFS processing algorithms, that appeared to bias the global means upward. Siegel et al. (2000) have shown that iterative methods to derive chlorophyll-dependent NIR water-leaving radiances substantially reduce the number of excessively large chlorophyll values especially at large concentrations. Also, the Ocean Chlorophyll-2 (OC2) bio-optical algorithm (O'Reilly et al., 1998), which utilizes the ratio of water-leaving radiances at 490 nm to that at 555 nm, is insensitive to the low chlorophyll concentrations found in the oceanic central gyres, and thus again biases the results high.

An accurate ocean color data set is required if we are to make meaningful comparisons to a coupled numerical simulation model. Consequently, we obtained SeaWiFS Level-1A Global Area Coverage (GAC) data (4-km resolution) from the GSFC/DAAC. The SeaWiFS Sep. 1997 to Feb. 2000 archive was re-analyzed using standard methods for

calibration (NASA SeaWiFS Project Table 199902) and atmospheric correction (Gordon and Wang, 1994). Modifications were made to 1) iteratively estimate water-leaving radiance contributions to the NIR bands using Siegel et al. (2000), 2) apply the OC3 bio-optical algorithm (O'Reilly et al., 1998), which utilizes the ratio of 443 nm to 555 nm, and switches to a 510 nm to 555 nm ratio when the radiance at 510 nm exceeds that at 443 nm. Additional modifications included the application of spectral foam reflectance (Frouin et al., 1996), elimination of data when the solar zenith angle exceeded 70°, elimination of all chlorophyll values > 25 mg m^{-3}, and exclusion of data when the aerosol reflectance at 865 nm exceeded 0.02. This latter modification avoids excessive sun glint and optically thick aerosols, both of which produce inaccurate chlorophyll derivations.

These modifications appear to ameliorate the adverse effects on chlorophyll contained in the original processing effort. Re-analyzed SeaWiFS chlorophyll concentrations (Fig. 1) show a major reduction in global mean value compared to other comparable data sets, and more importantly, a reduction in the variance. This reduction in variance is especially indicative of an improvement since it is now in agreement with the CZCS and blended data sets, and suggests that the number of excessively large chlorophyll values is now more reasonable. NIR, bio-optical algorithm, and spectral foam reflectance modifications are included in the new re-processing of SeaWiFS data now underway by the SeaWiFS Project (C.R. McClain, personal communication, 2000).

2.2. Coupled Physical/Biogeochemical Model

The coupled global physical/biogeochemical/radiative model was based on Gregg (2000). The only modifications were the forcing by actual atmospheric conditions during the

SeaWiFS era, rather than the monthly climatologies used previously, the introduction of a new phytoplankton group, coccolithophores, and a parameterization of biological processes in sea ice. An overview of the coupled model interactions illustrates the application of actual monthly surface wind stresses and sea ice (near-real-time analyses from the NOAA/National Center for Environmental Prediction; NCEP) and sea surface temperature from the Reynolds optimal interpolation analyses (OISST: Reynolds and Smith, 1994) obtained from the GSFC/DAAC (Fig. 2). Unfortunately, actual surface shortwave forcing and cloud properties were not available yet for this period from the International Satellite Cloud Climatology Project, so we used monthly climatologies for surface shortwave flux (to determine mixed layer depths in the model and the circulation fields) and surface spectral irradiance (to drive phytoplankton growth). This is a major shortcoming in the simulation.

A second major modification to the Gregg (2000) model was the successful introduction of coccolithophores as a fourth phytoplankton functional group, in addition to the diatoms, chlorophytes, and cyanobacteria groups already present (Fig. 3). Chlorophytes are intended to represent flagellates, and the cyanobacteria are intended to represent pico-prokaryotes. The term successful introduction means that the group does not become extinct over the course of a four-year run, since in this model there are no refuge populations to numerically prevent extinction. In this model, if a phytoplankton group does not possess physiological, physical, or optical characteristics to enable it to find a niche, it is allowed to become extinct and the assumption is made that the characteristics are improperly defined or that additional characteristics are necessary for survival.

Coccolithophore physiological and physical characteristics identify them as a rapid sinking, moderate growing phytoplankton group that has an exceptional capability for

utilizing nitrogen (Fig. 4). The rapid sinking rate is a function of the density of their calcium carbonate exoskeletons. In this model their sinking rate varies as a function of their concentration

$$w_s(coc) = 1.111C(coc) + 0.291 \quad (1)$$

where w_s is the sinking rate in m d^{-1}, C is chlorophyll concentration, and the term coc indicates coccolithophores alone. Only coccolithophores exhibit a sinking rate dependence on concentration in this model. However, the sinking rates of all groups are adjusted for viscosity according to Stokes Law, which is parameterized by temperature (Gregg, 2000). The sinking rate of coccolithophores ranges from 0.3 m d^{-1} for low concentrations to a maximum of 1.2 m d^{-1} for large concentrations, which is consistent with observations (Fritz and Balch, 1996; Bonin et al., 1986). Their relative (to diatom) maximum growth rates are derived from comparative experiments by Brand et al. (1986; 1983) and Eppley et al. (1969). Light saturation information is derived from Perry et al. (1981). According to Eppley et al. (1969), nitrogen uptake by coccolithophores is about twice the efficiency of diatoms, leading to a half-saturation constant for nitrogen k_N of 0.5 (diatom k_N = 1 in this model). A similar adjustment to cyanobacteria is made to simulate improved nitrogen utilization as a function of their small size. Chlorophyte k_N is set to 0.8 to place them intermediate between coccolithophores and cyanobacteria at the lower end, and diatoms at the upper end. These group-dependent k_N's represent a change from the Gregg (2000) version where k_N = 1 for the three functional groups.

In this version biogeochemical processes in sea ice were parameterized. This adaptation was necessitated by lack of overwintering success by phytoplankton in the extreme northern and southern ranges of the model, resulting in depletion of populations. In the previous

model, phytoplankton populations became so depleted in the local winter that they could not recover during the growing season. In nature, phytoplankton exist in sea ice over winter, and then enter the ocean upon ice melt (Smith and Nelson, 1986), a process known as seeding. The parameterization applied here was to cease all biogeochemical processes in the presence of sea ice, and then resume when the ice disappears. The activity was modified by the percentage of sea ice present in a model grid cell.

As in Gregg (2000), the Ocean General Circulation Model (OGCM; Schopf and Loughe, 1995) was run for 5 years with climatological wind stresses, SST, and surface shortwave fluxes. Then the biogeochemical model was initialized with homogeneous fields of diatoms, chlorophytes, cyanobacteria, and coccolithophores, each set at 0.05 mg m^{-3} chlorophyll concentrations. Initial nitrate and silicate fields were taken from Conkright et al. (1994) annual means. The coupled model was run for 4 years with climatological surface wind stresses, SST, shortwave fluxes, sea ice, and atmospheric optical constituents to avoid initialization effects and achieve steady state. Finally the model was run from Apr. 1997 to Feb. 2000 using actual wind stresses, SST, and sea ice fields for the months and years in question. The stresses, sea ice, and SST's were averaged over each month to prevent perturbations to the GCM.

3. Results and Discussion

3.1. Climatological Phytoplankton Group Distributions

As in Gregg (2000), all phytoplankton groups were initialized as homogeneous fields (Fig. 5), both horizontally and vertically, and allowed to distribute in the global oceans as physical, optical, and biogeochemical conditions permit. Since this model has been adjusted

by adding a new phytoplankton group, coccolithophores, it is useful to observe resulting distributions produced by climatological forcing conditions before proceeding to the SeaWiFS era analyses. After 4 years of forcing the model with climatological wind stresses, SST's, sea ice, and atmospheric optical conditions, the four phytoplankton groups were distributed globally in June according to the prevailing conditions and inter-group competition (Fig. 6). Diatoms predominated in the high latitudes, equatorial upwelling areas, and coastal boundaries. They were most responsible for the spring bloom features observed in the North Pacific and Atlantic. Cyanobacteria/picoplankton predominated in the central ocean gyres. Chlorophytes/flagellates represent a transitional group that occupies the fringes of the equatorial upwelling regions, the sub-polar front in the Southern Hemisphere, and the northwestern Pacific Ocean. Coccolithophores had a patchy distribution, with major features in the North Atlantic Ocean, the Bering Sea, the western equatorial Pacific, the California upwelling region, and the southern sub-polar frontal region. Predominance of diatoms in the high latitudes (Maranon et al., 2000; Eynaud et al., 1999; Hardy et al., 1996) and sparseness in the central ocean gyres (Maranon et al., 2000; Goericke, 1998) has been previously reported.

The predominance of cyanobacteria/picoplankton in the mid-ocean gyres is well-established (Goericke, 1998; Itturiaga and Marra, 1988; Itturiaga and Mitchell, 1986; Glover, 1985). Hardy et al. (1996) found abundant flagellate populations in the southern Pacific sub-polar frontal region. Abundances of coccolithophores have been reported in a variety of locations, such as the northeast Atlantic Ocean near Iceland (Balch et al., 1996; Malin et al., 1993), the southern Atlantic sub-polar front (Eynaud et al., 1999), the Southern California Bight (Ziveri et al., 1995), the central and western tropical Pacific (Balch and

Kilpatrick, 1996), and the southern Pacific sub-polar front (Hardy et al., 1996). Bishop (1989) and Malin et al. (1993) have also noted the propensity of coccolithophores to gather at sub-polar frontal regions. Thus limited in situ observations of phytoplankton distributions are in qualitative agreement with the model results.

Diatom dominance of the equatorial Pacific is counter to observations in the region, e.g., Chavez, (1989); Landry et al. (1997); Brown et al. (1999), which indicate a pico-nano-plankton dominated community. These results suggest iron limitation, since diatoms appear to be especially subject to iron availability (Miller et al., 1991; Morel et al., 1991a; b; Price et al., 1994). Since this model does not contain explicit iron regulation, predominance by picoplankton cannot be reproduced. Thus the model produces a phytoplankton group population structure that is reasonable in the absence of iron limitation, and in a sense may support the large-scale extrapolation of the limited iron enrichment experiments.

3.2. Seasonal Comparison of Total Chlorophyll in the SeaWiFS Record

The SeaWiFS record of chlorophyll concentrations from Sep. 1997 to Feb. 2000 was averaged monthly to produce an illustration of seasonal distributions. Similarly, total chlorophyll outputs from the model were averaged daily over the same period. The comparison shows general correspondence between SeaWiFS and model-computed total chlorophyll (Fig. 7). Regions of low and high chlorophyll were matched, and the general characteristics of the seasonal cycle were in agreement. The high latitude regions, the North Atlantic and Pacific Oceans, and the Antarctic Ocean were characterized by a very wide seasonal range of chlorophyll, with a prominent and large local spring/summer bloom and a large die-off in local winter. Mid-latitude regions were characterized by a much smaller

seasonal signal, with local winter producing maximum values. The equatorial Pacific had virtually no seasonal signal in either the model or SeaWiFS. The equatorial Atlantic had a modest seasonal signal, with a maximum in mid-to-late summer, and minima in spring and fall in SeaWiFS. The model agreed with the late summer maximum and the early spring minimum, but does not exhibit a fall secondary minimum. The tropical Indian Ocean was lowest in mid-spring and highest in mid-summer, which agreed with the model results. The North Indian Ocean seasonal signal was clearly dominated by the northwest monsoon in mid-winter, the even larger southwest monsoon in mid-to-late summer, and a minimum in chlorophyll associated with the inter-monsoon period. The model seasonal trends were in agreement with these results, but it underestimated the high chlorophyll values at the monsoon peaks. The southwest monsoon is a period of intense upwelling that produces elevated chlorophyll, but high winds associated with the monsoon also produce overlying absorbing aerosols that confound the SeaWiFS atmospheric correction algorithms and produce an overestimate of chlorophyll (Gregg, 2000). Still, the model did not appear to represent the extent of upwelling, which may be due to the absence of topographic and/or coastal influences.

Although the model exhibited an ability to simulate the seasonal distributions of chlorophyll as compared to SeaWiFS, there were some significant differences in timing and magnitude. In the North Pacific and Atlantic, the spring bloom peak occurred in the model in July and June, respectively. In SeaWiFS the bloom occurred in May in both basins, although it lingered through June in the North Pacific. This represents a departure from the CZCS climatology, when the peak occurred in June in both basins, although the North Pacific May values were nearly as large as the June values (Fig. 8). The mean May and

June SeaWiFS chlorophyll concentrations were about 1.6 times larger than the CZCS. In the model the bloom resulted from increased surface irradiance and mixed layer shoaling. Coupled with prevalent nutrients from winter mixed layer deepening and entrainment, this produced irradiance levels in the surface layer conducive to very large growth. The apparent delay in the model, and relative to the CZCS climatology, suggests that anomalous surface forcing was present in the two SeaWiFS spring/summers. Given that actual wind stresses and sea surface temperatures were used, it is possible that surface shortwave forcing and surface irradiance was larger and earlier in 1998 and 1999, possibly due to reduced cloud cover and thickness, that was not represented in the climatological conditions used in the model. The North Pacific also exhibited a pronounced fall bloom in SeaWiFS data that was not present in the model (Fig. 7). The CZCS climatology exhibited a similar feature (Fig. 8). Yoder et al. (1993) suggested that CZCS observations in the autumn above 40° N are unreliably high. While there may be bias associated with limited sampling and increasing solar zenith angle, the dynamics producing a fall bloom (convective overturn and replenishment of nutrients) are well-grounded in physical and biogeochemical principles. In the model nutrient replenishment was inadequate to compensate for diminished irradiance availability, especially given the deeper mixed layer. In reality, there may be influences related to eddy-forced isopycnal adjustment (e.g., Siegel et al., 1999), or diurnal variability of mixed layer depths.

3.3. Interannual Comparison of Total Chlorophyll in the SeaWiFS Record

The 2.5-year SeaWiFS chlorophyll record was generally dominated by the seasonal signal, but interannual variability is also readily apparent (Fig. 9). Perhaps the most dominant event

since the launch of SeaWiFS was the record El Niño and La Niña events in the tropical Pacific and Indian Oceans. The El Niño was underway in Sep. 1997 when SeaWiFS was launched, and continued (as indicated by anomalously high surface temperatures) until May 1998. Temperatures exceeded 4° above normal during the 1997-1998 event (Murtugudde et al., 1999). The high surface temperatures were the result of an eastward-propagating Kelvin wave, which was in turn induced by a reduction in westward winds along the tropical Pacific. This Kelvin wave suppressed the normally present upwelling conditions and shut down supply of nutrients to the surface. The result was vastly reduced chlorophyll concentrations. Low chlorophyll concentrations were readily apparent in the SeaWiFS tropical basin means from launch until early 1998 (Fig. 9). Similar low chlorophyll was represented in the model basin means. However, there were some discrepancies between the computed response to El Niño and the actual response as indicated by the SeaWiFS observations. SeaWiFS reached a minimum in chlorophyll in Dec. 1997 and apparently began to recover through early 1998. The model obeyed the OISST record, which showed that the El Niño did not end until May 1998. Murtugudde et al. (1999) suggested that local wind bursts beginning in March 1998 produced a local bloom in SeaWiFS data near 165° E. However, the basin-wide results here were the result of different processes. Beginning in Dec. 1997, westward wind stresses at the formation of the North Equatorial current developed (at about 120-150° W, 10-20° N). Over the course of the next few months, these wind stresses produced larger chlorophyll concentrations in the southeastern portion of the North Central Pacific in the model that appeared to spread over the equatorial counter current, eventually joining with a local bloom in the western tropical Pacific in Jan.-Feb. 1998 (Fig. 10). This sequence appears to be represented SeaWiFS. However, the disparity

in the basin means occurred by continued depletion of chlorophyll in the southern portion of the Peru current in the model (Fig. 10). In the model this was the result of poleward spreading of the El Niño Kelvin wave. SeaWiFS data indicated early depletion of chlorophyll in this region and no further reduction. One of the most notable features of the midst of the El Niño was the prominent expression of the equatorial counter current in SeaWiFS data. It was not as obvious in the model since the contrast in the color scale is not as apparent, but one can still observe its appearance (Fig. 10). This striking expression was likely due to reduced baroclinic shear between the equatorial counter current and the south equatorial current.

The La Niña condition prevalent in this region from May 1998 to the present was represented in the SeaWiFS data and the model (Fig. 9). Both indicated elevated chlorophyll concentrations, resulting from enhanced upwelling and supply of nutrients to the surface. Both indicated about a factor of 2 increase from the low point of the El Niño to the La Niña (Fig. 9). Re-establishment and intensification of upwelling conditions due to La Niña are shown in Fig. 11.

The expression of the El Niño in the tropical Indian Ocean was also one of the significant interannual signals observed by SeaWiFS. Anomalous upwelling in the eastern Indian Ocean was present in both the SeaWiFS data and the model in November 1997 (Fig. 10). This upwelling was induced by abnormally high wind stresses which produced abnormally low SST indicative of upwelling. In the model and SeaWiFS, this condition reversed and resulted in a steady reduction of surface chlorophyll in the equatorial Indian basin until the end of the El Niño in May 1998, when a more normal seasonal cycle began to assert itself. The departure of model chlorophyll from SeaWiFS in summer of 1998 and 1999 may have

be influenced by atmospheric correction difficulties in SeaWiFS associated with dust plumes accompanying the high winds of the southwest monsoon. Massive areas of the Arabian Sea failed the aerosol optical thickness criterion for SeaWiFS during these periods (Fig. 11). The absorbing nature of these aerosols resembles chlorophyll in the correction procedures. Although algorithm failure did not occur in the equatorial Indian monthly means, excessively large chlorophyll values are an expected result in the presence of sub-threshold aerosol optical thicknesses. Most of the increase in chlorophyll in the equatorial Indian in July and August occurred on the western side, closest to the dust source (Fig. 11). Similar large chlorophyll concentrations were retrieved from SeaWiFS during these months for the North Indian and equatorial Atlantic Oceans, suggesting a similar phenomenon. Some of the effect was most likely natural, resulting from upwelling induced by the southwest monsoon, but it is difficult to quantify. The model may be inhibited from exhibiting the large dynamic range in chlorophyll because of the lack of topographic and coastal influences.

A time series of nitrate distribution (Fig. 12) illustrates the dramatic effects of El Niño and La Niña. Nitrate concentrations were suppressed in Nov. 1997 in the tropical Pacific, but upwelling was strongly indicated in the eastern tropical Indian basin. By May the nitrate depletion in the tropical Pacific reached its minimum, and within one month reversed indicating the onset of La Niña. Murtugudde et al. (1999) observed a 6° change in temperature between May and Jun. 1998. By Aug. 1999 La Niña was firmly entrenched in the tropical Pacific. Chavez et al. (1999) measured 0.05 μM nitrate at 0° 155°W in Nov. 1997, which was lower than the corresponding model value of 0.5 μM, but which represents a significant departure from normal when 5 μM is a common value.

The North Central Pacific Ocean appeared to exhibit interannual variability related to the El Niño (Fig. 9), with lower peak values in the SeaWiFS data in winter/spring 1998 than in 1999. This was accompanied by anomalously high SST's along the California coast in spring 1998, which was indicative of reduced upwelling. The model indicated reduced upwelling along the California coast in spring 1998 as well, but overall the basin mean values in the model did not exhibit effects related to the El Niño.

The North Pacific and Atlantic basins exhibited very large interannual variability during the 2.5 years of SeaWiFS chlorophyll data collection (Fig. 9). The spring/summer bloom in the North Pacific in 1999 was much larger, although slightly later, than in 1998 in the SeaWiFS record. In the model, the formation of the bloom was tracked to mid-May 1999, with larger chlorophyll concentrations than in 1998. Then the bloom did not advance through June, and finally resumed briefly in July 1999. The net effect of this start-and-stop process in the model was a reduced total bloom magnitude. The cause of the discrepancy is most likely monthly averaging of the wind stresses. Anomalously low wind stresses in April and May 1999 provided rapid mixed layer shoaling. The mean winds of June were much higher, and the mixed layer shoaling slowed down. The mixed layer depth on May 5, 1998 was 70 m compared to 50 m in 1999. By July 4 the mixed layer depth was about 16 m both years, indicating a faster shoaling in 1998 than 1999. Actual daily wind stresses continued at low values through the end of May and into the beginning of June, producing continued mixed layer shoaling as suggested by the SeaWiFS observations. The slow down of mixed layer shoaling in the model allowed herbivore populations to keep pace with phytoplankton growth, and reduce the magnitude of the overall bloom. Use of climatological shortwave radiation and irradiance may also contribute to the discrepancy.

The North Atlantic showed an interannual maximum in spring/summer 1998 compared to 1999 in the SeaWiFS record, in contrast to the North Pacific (Fig. 9). In the North Atlantic, the model represented these interannual characteristics. In the model, the reduction in the spring bloom in 1999 was due to the rate at which the MLD shoals. It took about 60 days to shoal from 100 m to 30 m in 1998, as compared to 90 days in 1999 (and similarly in 1997, incidentally). This slow down in shoaling, as in the North Pacific, allowed herbivore populations to keep up with phytoplankton populations, and thus restrict their ability to maximize use of available nutrients. A result of this was that large phytoplankton populations were sustained longer in 1999 than in 1998 because grazing inhibited their use of nutrients.

The model tracked the SeaWiFS chlorophyll record in the North Central Atlantic, except for a 6-month period beginning in Oct. 1998 and lasting until Mar. 1999, when elevated SeaWiFS values predominated (Fig. 9). After this time the SeaWiFS data fell back to agreement with the model. The elevated SeaWiFS data for the basin were caused by very high chlorophyll values off the coast of Mauritania during this period (Fig. 11). Values exceeded 1.0 mg m^{-3} over large areas near the coast for several months. The model had a much smaller indication of large chlorophyll in this region. Wind stresses were from the east during this period but not anomalously so, and SST data did not exhibit cool anomalies that would indicate upwelling until March 1999, when the model also indicated elevated chlorophyll values here. This suggests the possibility of a Saharan dust episode producing inaccurate SeaWiFS chlorophyll data, but there appeared to be no similar expression in the equatorial Atlantic. We also do not presently have confirmation from SeaWiFS derived aerosol optical thickness estimates that a Saharan dust outbreak occurred and there is also

little evidence of algorithm failure that usually accompanies such events. Furthermore, a confirmed intense outbreak in Feb. 2000 did not produce SeaWiFS chlorophyll values that deviate from the model greatly (Fig. 9, 13).

The equatorial Atlantic exhibited such a large amount of interannual variability in SeaWiFS data that the seasonal signal was sometimes obscured (Fig. 9). The model did not track the wide interannual variability of the SeaWiFS record, and appeared to stay on the seasonal course, although it was always within the SeaWiFS standard deviation. This region is subject to several influences that are not represented in the model, such as riverine inputs form the Amazon to the west and the Congo to the east, as well as several sources of error for SeaWiFS data (colored dissolved organic matter from the rivers, absorbing aerosols). The most conspicuous departure occurred in Jul. 1999 and lasted until Sep. 1999, when SeaWiFS produced much larger chlorophyll estimates than the model. A band of very high chlorophyll formed along the equatorial axis in Jul. 1999 (Fig. 13). This high chlorophyll was suggestive of upwelling, but there was no correspondence in the OISST data, nor were wind stresses anomalous. Congo River outflow reaches a seasonal maximum in Jul. and Aug. (Signorini et al., 1999), which provides the simplest explanation. The high chlorophyll concentrations diminished for the remainder of the year, then re-appeared in Jan. 2000, although now it was localized to the coast suggesting riverine influence, most likely due to the increased outflow of the Congo that tends to begin in January (Signorini et al., 1999).

The Southern Hemisphere basins appeared to exhibit very little interannual variability in either the SeaWiFS or model representations of chlorophyll, and the two were in overall agreement (Fig. 9). The model tended to underestimate SeaWiFS concentrations in the austral winter in the Antarctic, but this may be due to the 72° solar zenith angle limit on data

collection for SeaWiFS. The limit selectively excludes data under low irradiance, where primary production is low and chlorophyll abundances are also expected to be low, as indicated by the model which has no such bias. In fact, where slivers of SeaWiFS data exist, the values appeared to be low and more in agreement with the model (Fig. 11, 13). A similar pattern emerged in the North Pacific and Atlantic basins. The model appeared to overestimate chlorophyll in austral summer, which may be due to iron limitation.

3.3. Interannual Variability in Phytoplankton Group Distributions

Phytoplankton group distributions exhibited significant departures from climatological conditions in some basins during the 2.5-year SeaWiFS record. These observations are difficult to confirm with in situ observations, because of how recent the SeaWiFS observations are, and how sparse phytoplankton group data can be. Nevertheless, the model results can provide some insight into the mechanisms governing basin-scale phytoplankton group changes, and can provide hypotheses as to the nature if interannual variability.

The largest interannual variability in phytoplankton distributions occurred in the equatorial Pacific and Indian Oceans, where the El Niño and La Niña events were most prominent. In the tropical Pacific, diatom populations diminished as the El Niño persisted, reaching a minimum at the nominal end of the event in May 1998 (Fig. 14). During this time, diatoms were replaced by largely coccolithophores, but also a mixture of chlorophytes and cyanobacteria. With the end of the El Niño and the beginning of the La Niña, diatom relative abundance increased and eventually reached a larger proportion than before the El Niño. These results conform to observations by Chavez et al. (1999), who noted that in the tropical Pacific, El Niño is dominated by pico and nano plankton, and the La Niña brings

about the increased relative abundance of diatoms. In the model this was because enhanced nutrient supply provided by intensified upwelling of La Niña favored the faster growing diatoms. With the relatively rapid sinking rates, the reduced nutrient availability in El Niño was insufficient for them to maintain their populations, and the slower growing but slower sinking cyanobacteria and chlorophytes attained a competitive advantage. Coccolithophores sink relatively rapidly but their ability to scavenge nutrients with greater efficiency than diatoms gave them an advantage in El Niño.

A different pattern emerged from the El Niño in the tropical Indian Ocean. Here the main effect of El Niño was to produce intensified upwelling in the eastern portion of the basin (Fig. 14). Although the pattern of phytoplankton group relative abundance was dissimilar from the Pacific, the same biological and physical principles are at work. Thus the increased upwelling in the Indian Ocean produced greater nutrient supply, and diatom populations increased their abundances relative to the other groups (Fig. 14). Re-establishment of more normal circulation patterns arriving with La Niña resulted in diminishing diatom populations, and the increase of coccolithophores and cyanobacteria (Fig. 14). An interesting observation is that coccolithophores appear to have increased their abundances relative to cyanobacteria during La Niña.

In the North Atlantic, diatoms predominated throughout the SeaWiFS record, with cyanobacteria and then coccolithophores exchanging secondary relative abundance as winter approached (Fig. 14). The exceptional spring/summer peak in 1998 exhibited slightly increased relative abundance of coccolithophores. The smaller bloom of 1999 had slightly more diatoms and slightly less coccolithophores and chlorophytes.

The central North Pacific exhibited little interannual variability, as did the total chlorophyll record (Fig. 14). Instead it indicated a pattern of diatom predominance in early spring, yielding to cyanobacteria predominance in summer and late fall. Coccolithophore relative abundances increased in the boreal winter and decreased in late summer in a pattern that was out of phase with diatoms and cyanobacteria.

4. Conclusions

The 2.5-year SeaWiFS mission has given us our first comprehensive glimpse of interannual variability of ocean chlorophyll dynamics. Moreover, it was launched as one of the largest El Niño events was underway, and which eventually gave way to one of the largest, most intensive, and longest-lasting La Niña events ever recorded. The SeaWiFS chlorophyll record captures the response of ocean phytoplankton to these significant events in the tropical Indo-Pacific basins, but also indicates significant interannual variability unrelated to the El Niño/La Niña. This includes large variability in the North Atlantic and Pacific basins, large variability in the North Central and equatorial Atlantic, and milder patterns in the North Central Pacific, the latter of which may be due partially to the El Niño. The Southern Hemisphere exhibits, in contrast, relatively little interannual variability during the SeaWiFS record.

We are fortunate to live in an era when global atmospheric data sets are routinely and nearly immediately available. Thus we have the opportunity to drive a coupled physical/biogeochemical/radiative model of the global oceans with actual near-real-time forcing data such as wind stresses, SST's, and sea ice. Our only limitation is cloud cover and thickness data, which are necessary to evaluate the shortwave flux, which affects mixed

layer dynamics, and the spectral irradiance with depth, which drives phytoplankton dynamics. Although this is a major shortcoming, the availability of the other forcing data gives us an opportunity to track the SeaWiFS record with a global coupled model and attempt to provide physically and biogeochemically meaningful explanations of the variability observed in the SeaWiFS data set.

Even without cloud data, the coupled model was able to represent the seasonal distributions of chlorophyll during the SeaWiFS era, and was capable of differentiating among the widely different processes and dynamics occurring in the global oceans. The model was also reasonably successful in representing the interannual signal, especially when it was large, such as the El Niño and La Niña events in the tropical Pacific and Indian Oceans. In these two regions the model provided different phytoplankton group responses for the different events. The interannual variability in the North Atlantic, which was exhibited in SeaWiFS data as a decline in the spring/summer bloom in 1999 relative to 1998 was represented, and resulted in the model from a more slowly shoaling mixed layer, allowing herbivore populations to increase at a faster rate thus preventing maximum and immediate utilization of available nutrients from winter convection. However, several aspects of the interannual cycle were not well-represented by the model. Some of which may be due to the application of monthly averaged winds such as the North Pacific, some by the model deficiencies of a lack of topographic and coastal influences such as the North Indian Ocean, some may be related to the lack of monthly cloud data, some may be due to riverine influences missing in the model such as the equatorial Atlantic, and finally some may be the result of biases in SeaWiFS atmospheric correction procedures such as absorbing aerosols which are common in the equatorial and mid-latitude eastern Atlantic

and the North and equatorial Indian Oceans. Nevertheless, broad agreement suggests confidence in the large scale (synoptic and basin scale) processes in the model and its ability to provide plausible explanations for some the variability observed in this unique spaceborne data set.

Acknowledgements

Development of the OGCM was by Paul Schopf, George Mason University Center for Ocean-Land-Atmospheres. The NASA/GSFC/DAAC provided the CZCS and SeaWiFS data that was used for comparison, and access to near-real-time NCEP wind stresses and sea ice data, and OI SST data. This work was supported under NASA Grant (RTOP) 971-622-51-31.

References

Balch, W.M., K.A. Kilpatrick, 1996. Calcification rates in the equatorial Pacific along 140° W. Deep-Sea Research 43, 971-993.

Balch, W.M., K.A. Kilpatrick, and C.C. Trees, 1996. The 1991 coccolithophore bloom in the central North Atlantic. 1. Optical properties and factors affecting their distribution. Limnology and Oceanography 41, 1669-1683.

Bishop, J.K.B., 1989. Regional extremes in particulate matter composition and flux: effects on the chemistry of the ocean interior. In: Productivity of the ocean: past and present, W.H. Berger, V.S. Smetacek, and G. Wefer, editors, Wiley, New York, pp. 117-137.

Bonin D.J., M.R. Droop, S.Y. Maestrini, and M.-C. Bonin, 1986. Physiological features of six micro-algae to be used as indicators of seawater quality. Cryptogamie, Algologie 7, 23-83.

Brand, L.E., W.G. Sunda, and R.R.L. Guillard, 1986. Reduction of marine phytoplankton reproduction rates by copper and cadmium, Journal of Experimental Marine Biology and Ecology 96, 225-250.

Brand, L.E., W.G. Sunda, and R.R.L. Guillard, 1983. Limitation of marine phytoplankton reproductive rates by zinc, manganese, and iron. Limnology and Oceanography 28, 1182-1198.

Brown, S.L., M.R. Landry, R.T. Barber, L. Campbell, D.L. Garrison, and M.M. Gowing, 1999. Picophytoplankton dynamics and production in the Arabian Sea during the 1995 southwest monsoon. Deep-Sea Research 46, 1745-1768.

Chavez, F.P., P.G. Strutton, G.E. Friederich, R.A. Feely, G.C. Feldman, D.G. Foley, and M.J. McPhaden, 1999. Biological and Chemical Response of the Equatorial Pacific to the 1997-98 El Niño. Science 286, 2126-2131.

Chavez, F.P., 1989. Size distribution of phytoplankton in the central and eastern tropical Pacific. Global Biogeochemical Cycles 3, 27-35.

Conkright, M.E., S. Levitus and T.P. Boyer, 1994. World Ocean Atlas, Volume 1: Nutrients, NOAA Atlas NESDIS 1, 150 pp.

Conkright, M.E. and W.W. Gregg, 2000. Comparison of chlorophyll climatologies: in situ, CZCS, blended in situ-CZCS, and SeaWiFS. Global Biogeochemical Cycles, submitted.

Dutkiewicz, S., M. Follows, J. Marshall, and W.W. Gregg, 2000. Interannual variability of phytoplankton abundances in the North Atlantic. Deep-Sea Research, in press.

Eppley, R.W., J.N. Rogers, and J.J. McCarthy, 1969. Half-saturation constants for uptake of nitrate and ammonium by marine phytoplankton. Limnology and Oceanography 14, 912-920.

Eynaud, F., J. Girardeau, J.-J. Pichon, and C.J. Pudsey, 1999. Sea-surface distribution of coccolithophores, diatoms, silicoflagellates, and dinoflagellates in the South Atlantic Ocean during the late austral summer 1995. Deep-Sea Research 46, 451-482.

Feldman, G.C., N. Kuring, C. Ng, W. Esaias, C.R. McClain, J. Elrod, N. Maynard, D. Endres, R. Evans, J. Brown, S. Walsh, M. Carle, and G. Podesta, 1989. Ocean color: Availability of the global set. Eos Transactions of the AGU, 70, 634-641.

Fritz, J.J. and W.M. Balch, 1996. A continuous culture study of Emiliana huxleyi: Determination of coccolith detachment rates and the relevance to cell sinking rates. Journal of Experimental Marine Biology and Ecology 207, 127-147.

Frouin, R., M. Schwindling, and P.-Y. Deschamps, 1996. Spectral reflectance of sea foam in the visible and near-infrared: In situ measurements and remote sensing implications. Journal of Geophysical Research 101, 14361-14371.

Glover, H.E., 1985. The physiology and ecology of the marine cyanobacterial genus *Synechococcus*. Advances in Microbiology 3, 49-107.

Goericke, R., 1998. Response of phytoplankton community structure and taxon-specific growth rates to seasonally varying physical forcing in the Sargasso Sea off Bermuda. Limnology and Oceanography 43, 921-935.

Gordon, H.R. and M. Wang, 1994. Retrieval of water-leaving radiance and optical thickness over the oceans with SeaWiFS: A preliminary algorithm. Applied Optics 33, 443-452.

Gregg, W.W., 2000. Seasonal distributions of global ocean chlorophyll and nutrients: Analysis with a coupled ocean general circulation, biogeochemical, and radiative model. Journal of Geophysical Research, submitted.

Gregg, W.W. and M.E. Conkright, 2000. Global seasonal climatologies of ocean chlorophyll: Blending in situ and satellite data for the CZCS era. Journal of Geophysical Research, submitted.

Gregg, W.W. and J.J. Walsh, 1992. Simulation of the 1979 spring bloom in the Mid-Atlantic Bight: A coupled physical/ biological/optical model. Journal of Geophysical Research 97: 5723-5743.

Hardy, J., A. Hanneman, M. Behrenfeld, and R. Horner, 1996. Environmental biogeography of near-surface phytoplankton in the southeast Pacific Ocean. Deep-Sea Research 43, 1647-1659.

Itturiaga, R. and B.G. Mitchell, 1986. Chrococcoid cyanobacteria: a significant component in the food web dynamics of the open ocean. Marine Ecology Progress Series 28, 291-297.

Itturiaga, R. and J. Marra, 1988. Temporal and spatial variability of chroccoid cyanobacteria *Synechococcus* spp. specific growth rates and their contribution to primary productivity in the Sargasso Sea. Marine Ecology Progress Series 44, 175-181.

Landry, M.R., R.T. Barber, R.R. Bidigare, F. Cahi, K.H. Coale, H.G. Dam, M.R. Lewis, S.T. Lindley, J.J. McCarthy, M.R. Roman, D.K. Stoecker, P.G. Verity, and J.R. White, 1997. Iron and grazing constraints on primary production in the central equatorial Pacific: An EqPac synthesis. Limnology and Oceanography 42, 405-418.

Malin, G., S. Turner, P. Liss, P. Holligan, and D. Harbour, 1993. Dimethylsulfide and dimethylsulphoniopropionate in the northeast Atlantic during the summer coccolithophore bloom. Deep-Sea Research 40, 1487-1508.

Maranon, E., P.M. Holligan, M. Varela, B. Mourino, and A.J. Bale, 2000. Basin-scale variability of phytoplankton biomass, production and growth in the Atlantic Ocean. Deep-Sea Research 47, 825-857.

McClain, C.R., M.L. Cleave, G.C. Feldman, W.W. Gregg, S.B. Hooker, and N. Kuring Science quality SeaWiFS data for global biosphere research. Sea Technology Sept., 10-16.

McGillicuddy, D.J., A.R. Robinson, and J.J.McCarthy, 1995. Coupled physical and biological modelling of the spring bloom in the North Atlantic (II): three dimensional bloom and post-bloom processes. Deep-Sea Research 8, 1359-1398.

Miller, C.B. and others, 1991. Ecological dynamics in the subarctic Pacific, a possibly iron-limited system. Limnology and Oceanography 36, 1600-1615.

Morel, F.M.M., R.J.M. Hudson, and N.M. Price, 1991a. Limitation of productivity by trace metals in the sea. Limnology and Oceanography 36, 1742-1755.

Morel, F.M.M., J.G. Rueter, and N.M. Price, 1991b. Iron nutrition of phytoplankton and its possible importance in the ecology of open ocean regions with high nutrient and low biomass. Oceanography 4, 56-61.

Murtugudde, R.G., S.R. Signorini, J.R. Christian, A.J. Busalacchi, C.R. McClain, and J. Picaut, 1999. Ocean color variability of the tropical Indo-Pacific basin observed by SeaWiFS during 1997-1998. Journal of Geophysical Research 104, 18351-18366.

O'Reilly, J.E., S. Maritorena, B.G. Mitchell, D.A. Siegel, K.L. Carder, S.A. Garver, M. Kahru, and C. McClain, 1998. Ocean color chlorophyll algorithms for SeaWiFS. Journal of Geophysical Research 103, 24937-24953.

Perry, M.J., M.C. Talbot, and R.S. Alberte, 1981. Photadaptation in marine phytoplankton: response of the photosynthetic unit. Marine Biology 62, 91-101.

Price, N.M., B.A. Ahner, and F.M.M. Morel, 1994. The equatorial Pacific Ocean: Grazer-controlled phytoplankton populations in an iron-limited ecosystem, Limnology and Oceanography 39, 520-534.

Reynolds, R.W. and T.M. Smith, 1994. Improved global sea surface temperature analyses using optimum interpolation. Journal of Climate 7, 75-86.

Sarmiento, J.L., R.D. Slater, M.J.R. Fasham, H.W. Ducklow, J.R. Toggweiler, and G.T. Evans, 1993. A seasonal three-dimensional ecosystem model of nitrogen cycling in the North Atlantic euphotic zone. Global Biogeochemical Cycles 7, 417-450.

Schopf, P.S. and A. Loughe, 1995. A reduced gravity isopycnal ocean model: Hindcasts of El Nino. Monthly Weather Review 123, 2839-2863.

Shimoda, H., 1999. ADEOS overview. IEEE Transactions on Geoscience and Remote Sensing 37: 1465-1471.

Siegel, D.A., M. Wang, S. Maritorena, and W. Robinson, 2000. Atmospheric correction of satellite ocean color imagery: The black pixel assumption. Applied Optics, submitted.

Siegel, D.A., D.J. McGillicuddy, and E.A. Fields, 1999. Mesoscale eddies, satellite altimetry, and new production in the Sargasso Sea. Journal of Geophysical Research 104, 13359-13379.

Signorini, S.R., R.G. Murtugudde, C.R. McClain, J.R. Christian, J. Picaut, and A.J. Busalacchi, 1999. Biological and physical signatures in the tropical and subtropical Atlantic. Journal of Geophysical Research 104: 18367-18382.

Smith, W.O. and D.M. Nelson, 1986. Importance of ice-edge phytoplankton production in the Southern Ocean. BioScience 36, 251-256.

Yoder, J.A., C.R. McClain, G.C. Feldman, and W.E. Esaias, 1993. Annual cycles of phytoplankton chlorophyll concentrations in the global ocean: a satellite view. Global Biogeochemical Cycles 7: 181-193.

Walsh, J.J., D.A. Dieterle, F.E. Muller-Karger, R. Bohrer, W.P. Bissett, R.J. Varela, R. Aparicio, R. Diaz, R. Thunell, G.T. Taylor, M.I. Scranton, K.A. Fanning, and E.T. Peltzer, 1999. Simulation of carbon-nitrogen cycling during spring upwelling in the Cariaco Basin, Journal of Geophysical Research 104, 7807-7825.

Ziveri, P., R.C. Thunell, and D. Rio, 1995. Seasonal changes in coccolithophore densities in the Southern California Bight during 1991-1992. Deep-Sea Research 42, 1881-1903.

Figure Captions

Fig. 1. Comparison of re-analyzed SeaWiFS global data with other global data sets. IS indicates the in situ archive maintained by NOAA/NODC, CZ indicates the CZCS, BL indcates a blended data set (Gregg and Conkright, 2000), SW indicates SeaWiFS data, and OC3 indicates the re-analyzed data using an NIR reflectance correction and the OC3 bio-optical algorithm. Top: Global means. Bottom: global variances. Figure is reprinted courtesy of M. Conkright, NOAA/NODC.

Fig. 2. Diagrammatic representation of the coupled circulation, biogeochemical, and radiative model of the global oceans. Monthly climatological wind and atmospheric optical properties are used to produce surface shortwave radiation and spectral irradiance fields. Near-real-time monthly means of wind stresses, SST's, and sea ice are used to drive the circulation and biogeochemical fields for the SeaWiFS record. Outputs from the model are spectral upwelling radiance, primary production (which is an explicit calculation derived from the growth functions), chlorophyll abundances for each of the phytoplankton groups, and nutrients (nitrate, ammonium, and silicate).

Fig. 3. Diagrammatic representation of the biogeochemical model. Four phytoplankton components, diatoms, chlorophytes (representing nanoflagellates), cyanobacteria (representing prokaryotic picoplankton), and coccolithophores interact with three nutrient components (nitrate, ammonium, and silicate), and contribute to detritus when ingested or upon death, which returns to the ammonium pool immediately and the nitrate pool later upon remineralization. Herbivores ingest phytoplankton groups non-preferentially, and contribute to the ammonium pool though excretion, and eventually the nitrate pool upon death and remineralization.

Fig. 4. Phytoplankton group biological and physical characteristics. Top left: Maximum growth rate. Top right: Maximum sinking rates. Coccolithophore rates are concentration-dependent, and shown here is a median value. Actual rates range from 0.3 to 1.2 m d^{-1}. Bottom left: Half-saturation constants for nitrogen utilization (k_N). Bottom right: Light saturation parameters, I_k. Low light is defined as < 50 μ moles photons m^{-2} s^{-1}, medium light is 50-200, and high light is > 200.

Figure 5. Initial surface conditions for the 4 functional phytoplankton groups in the coupled model (mg m^{-3}). Distributions with depth are the same as shown here.

Figure 6. Phytoplankton group distributions computed for June after 4 years of simulation. These represent values for a single day near the beginning of the month and not monthly means.

Fig. 7. Comparison of model-generated mean chlorophyll (solid line) with climatological monthly mean SeaWiFS chlorophyll by oceanographic basin. Error bars on the SeaWiFS chlorophyll means represent one-half the SeaWiFS standard deviation. SeaWiFS climatological monthly means are derived by averaging over the 2.5-year record. Model means are averaged daily over the 2.5-year period.

Fig. 8. CZCS climatological monthly mean pigment for the North Pacific and North Atlantic basin. The spring/summer peak pigment values occurred in June for both basins, although in the North Pacific the May concentration was nearly as large as the June.

Fig. 9. Comparison of model daily chlorophyll (solid line) with monthly mean SeaWiFS chlorophyll by oceanographic basin for the 2.5-year SeaWiFS record. Error bars on the SeaWiFS chlorophyll means represent one-half the SeaWiFS standard deviation.

Fig. 10. Top: Mean monthly model chlorophyll for November 1997 compared with SeaWiFS data. Bottom: February 1998. This shows the evolution of the El Niño in the equatorial Pacific and Indian Oceans. Note suppressed chlorophyll concentrations in the equatorial Pacific and increased concentrations in the eastern equatorial Indian.

Fig. 11. Top: Mean monthly model chlorophyll for August 1998 compared with SeaWiFS data. Bottom: March 1999. By August 1998 the La Niña is well-established and is indicated by high chlorophyll concentrations in the equatorial Pacific. In March 1999 an

intense bloom of chlorophyll appears off the coast of Mauritania in the North Central Atlantic in the SeaWiFS data. The model indicates this but not as intensely. This sequence of images also illustrates seasonal variability. The vestiges of the austral summer bloom in the Antarctic are clearly apparent in the model, and sometimes agrees with SeaWiFS, but appear to overestimate especially in the southeast portion of the Pacific sector.

Fig. 12. This sequence of images illustrates the dramatic effects of El Niño and La Niña in model nitrate concentrations. In November 1997 high nitrate values in the eastern equatorial Indian occur as a result of intense upwelling. Nitrate concentrations continue to diminish through May 1998 in the tropical Pacific, and then begin to re-establish upwelling conditions in June 1998 as the La Niña develops. By September 1999 the La Niña is fully established. Seasonal variability is also apparent in the sequence. Note the exhaustion of nitrate in the North Pacific and Atlantic in November 1997 and September 1998, as the result of phytoplankton growth in the boreal summer. Replenishment occurs by May 1998. A much smaller seasonal signal is also apparent in the southern ocean.

Fig. 13. Top: Mean monthly model chlorophyll for July 1999 compared with SeaWiFS data. Bottom: February 2000. In July 1999 an intense bloom of chlorophyll has developed in the equatorial Atlantic. A similar feature appears in the model but not as intense. Similar patterns of high latitude blooms are observed in the Northern Hemisphere. By February 2000 more normal chlorophyll patterns have arrived, but with possibly continued exceptional upwelling. A severe dust storm was observed in SeaWiFS and AVHRR data off the Sahara Desert, and may be causing the large chlorophyll concentrations off Mauritania.

Fig. 14. Phytoplankton group distributions during the SeaWiFS record in 4 basins. Top left: Equatorial Pacific, where diatoms predominate the La Niña period but not the El Niño. Top right: Equatorial Indian, where diatoms predominate the El Niño, but other groups predominate in the La Niña. Note the predominance of coccolithophores. Bottom left: North Atlantic, showing overall diatoms predominance but shifts in late summer to cyanobacteria and winter to coccolithophores. Bottom right: North Central Pacific, which exhibits little compositional change as a function of interannual variability.

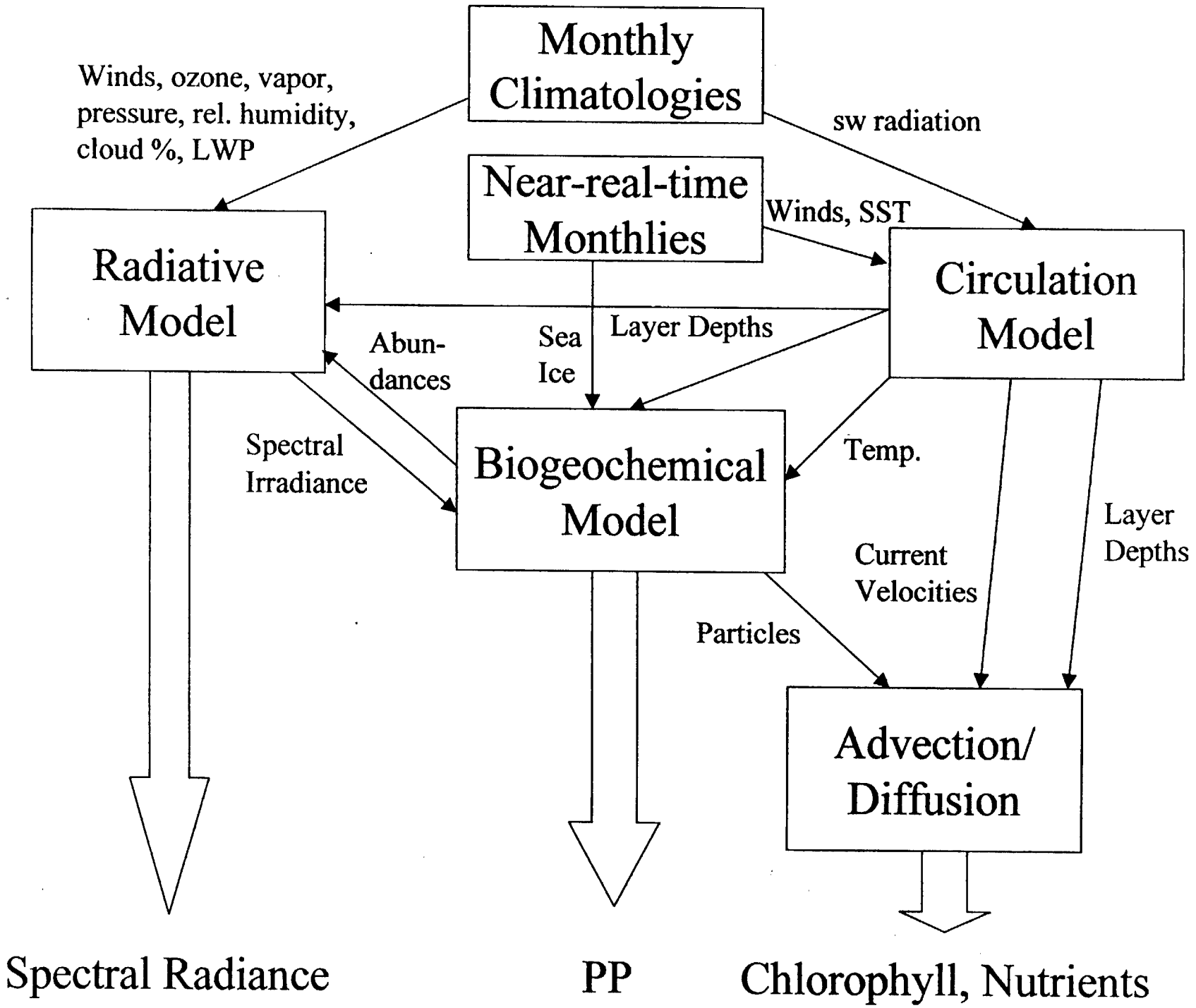
Monthly Climatologies
Winds, ozone, vapor, pressure, rel. humidity, cloud %, LWP
sw radiation
Near-real-time Monthlies
Winds, SST
Radiative Model
Circulation Model
Abun-dances
Sea Ice
Layer Depths
Spectral Irradiance
Biogeochemical Model
Temp.
Layer Depths
Current Velocities
Particles
Advection/ Diffusion
Spectral Radiance
PP
Chlorophyll, Nutrients

Global Chlorophyll Means

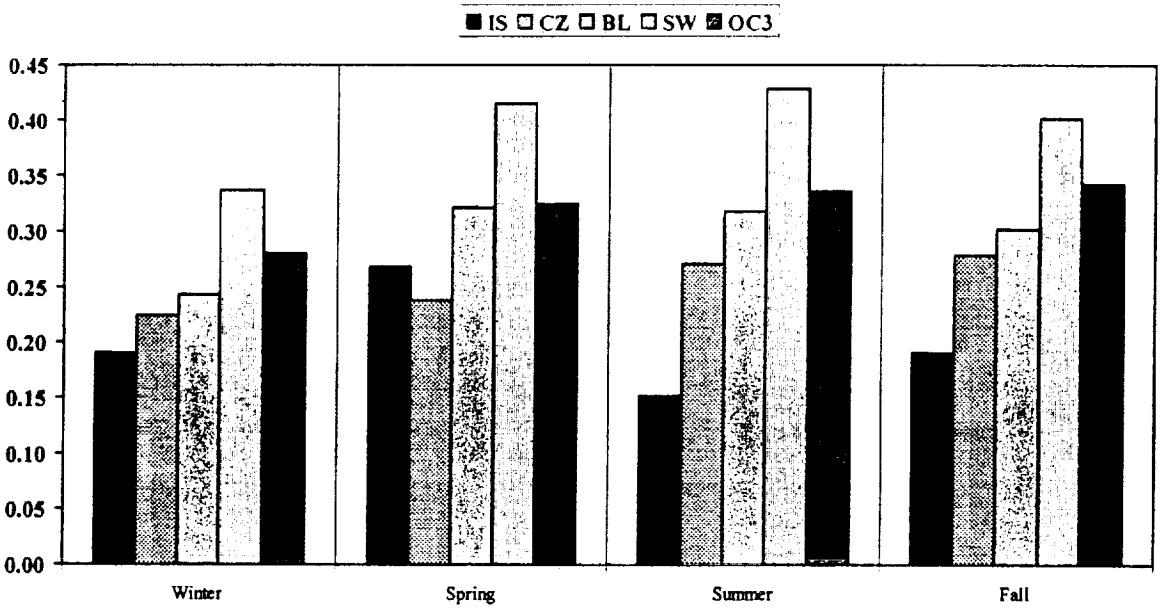

Global Chlorophyll Variances

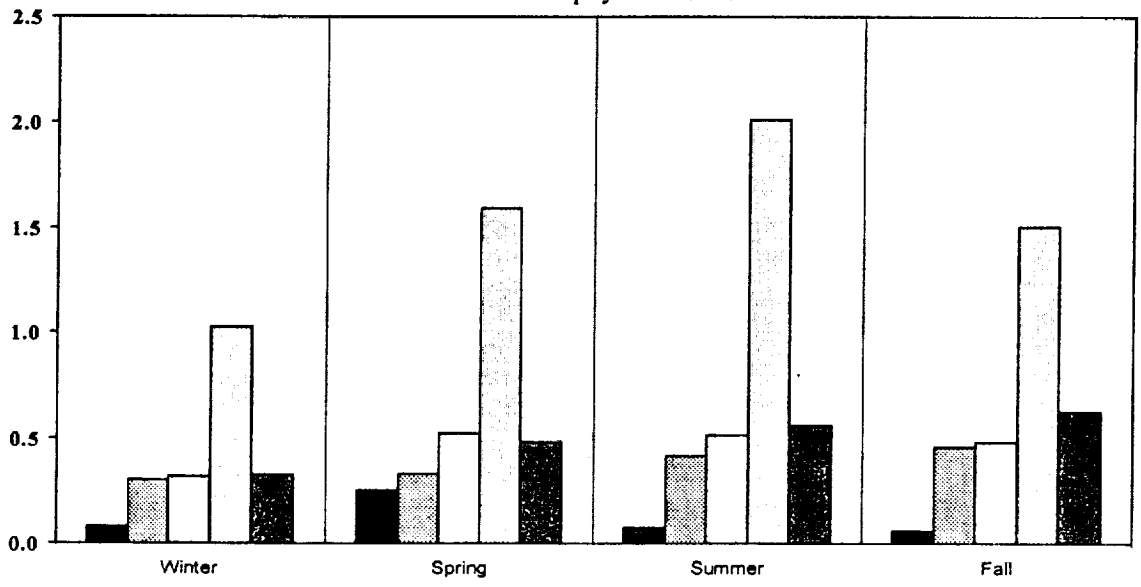

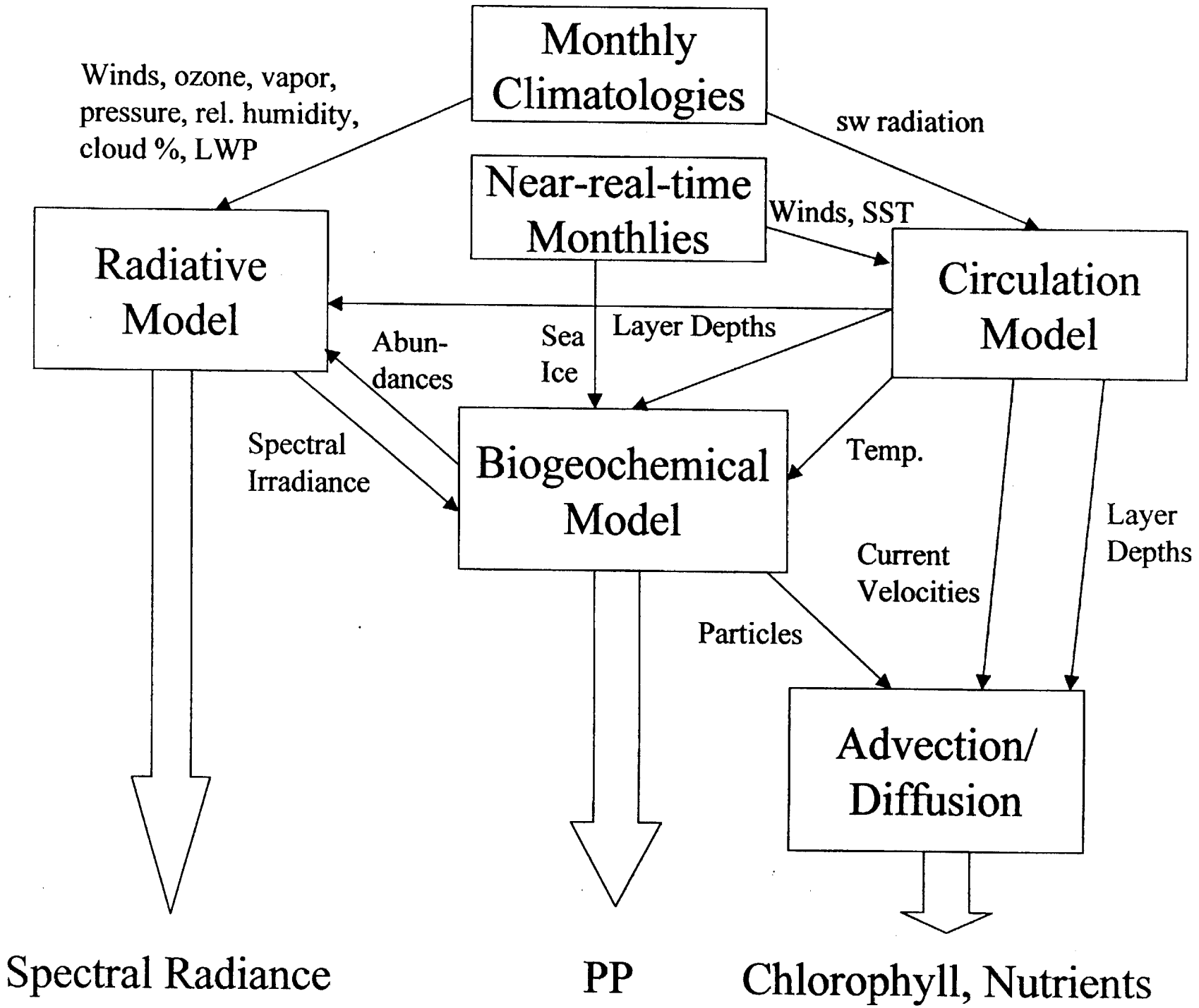
Monthly Climatologies
Winds, ozone, vapor, pressure, rel. humidity, cloud %, LWP
sw radiation
Near-real-time Monthlies
Winds, SST
Radiative Model
Circulation Model
Abun-dances
Sea Ice
Layer Depths
Spectral Irradiance
Biogeochemical Model
Temp.
Layer Depths
Current Velocities
Particles
Advection/ Diffusion
Spectral Radiance
PP
Chlorophyll, Nutrients

Biological Model

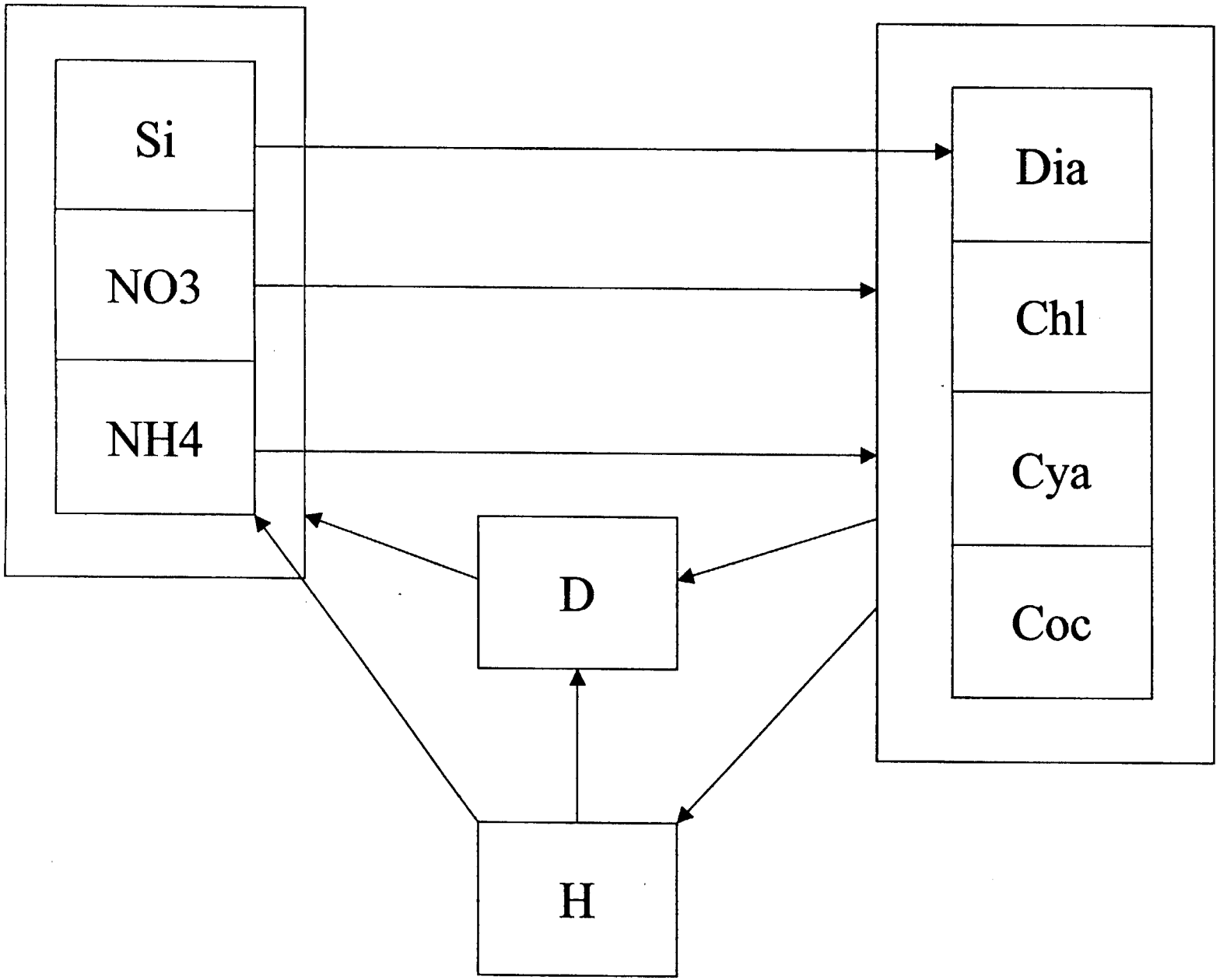

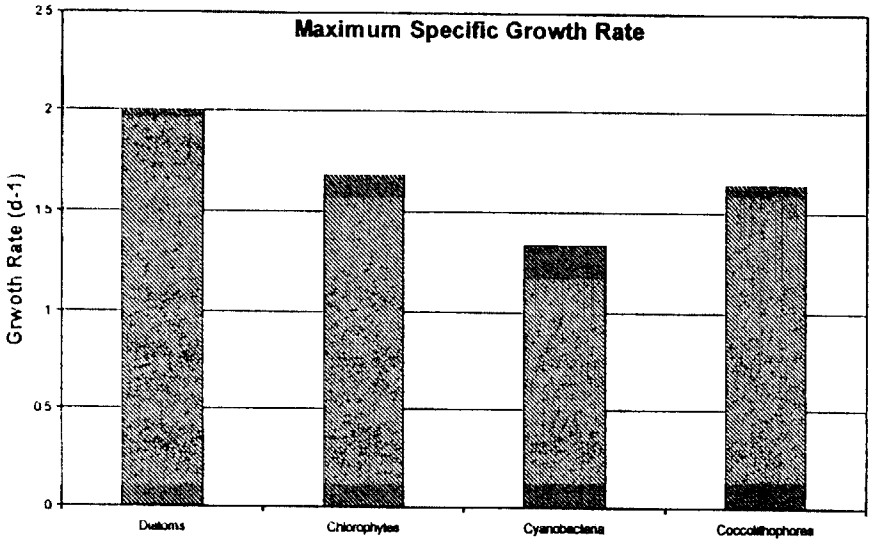
Maximum Specific Growth Rate
Grwoth Rate (d-1)
2.5
2
1.5
1
0.5
0
Diatoms
Chlorophytes
Cyanobacteria
Coccolithophores

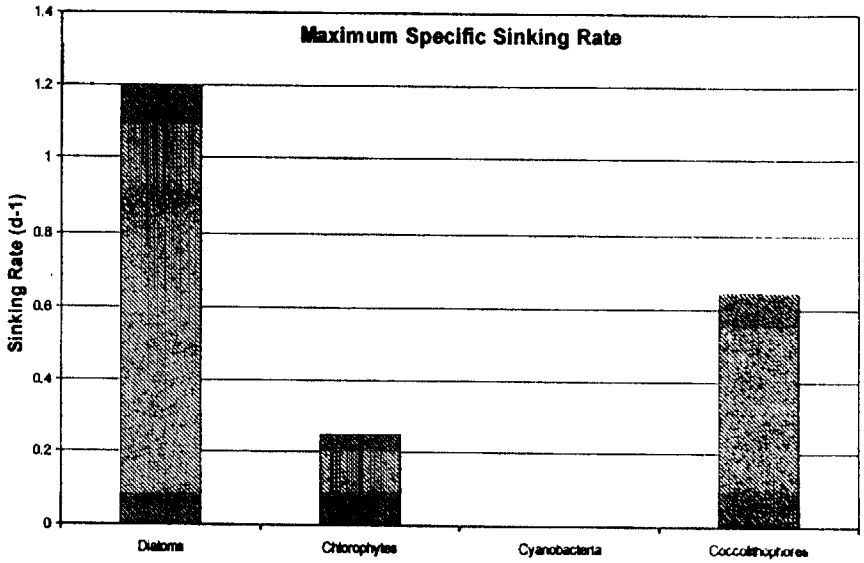
Maximum Specific Sinking Rate
Sinking Rate (d-1)
1.4
1.2
1
0.8
0.6
0.4
0.2
0
Diatoms
Chlorophytes
Cyanobacteria
Coccolithophores

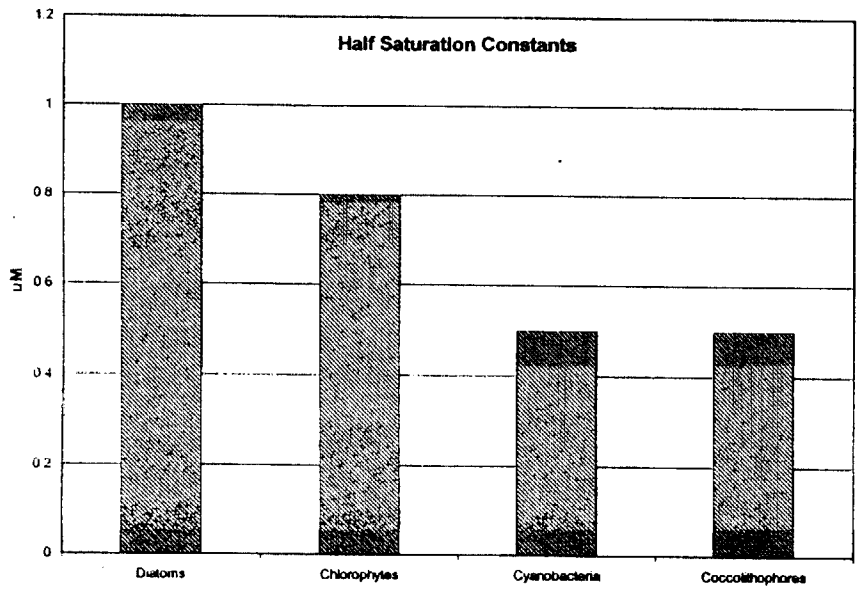
Half Saturation Constants
µM
1.2
1
0.8
0.6
0.4
0.2
0
Diatoms
Chlorophytes
Cyanobacteria
Coccolithophores

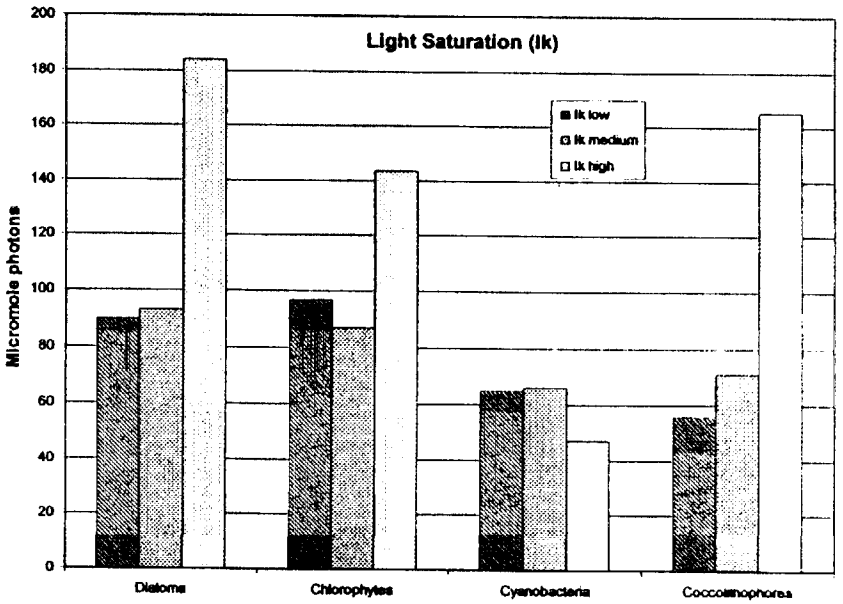
Light Saturation (Ik)
Micromole photons
200
180
160
140
120
100
80
60
40
20
0
Ik low
Ik medium
Ik high
Diatoms
Chlorophytes
Cyanobacteria
Coccolithophores

Diatoms

Chlorophytes

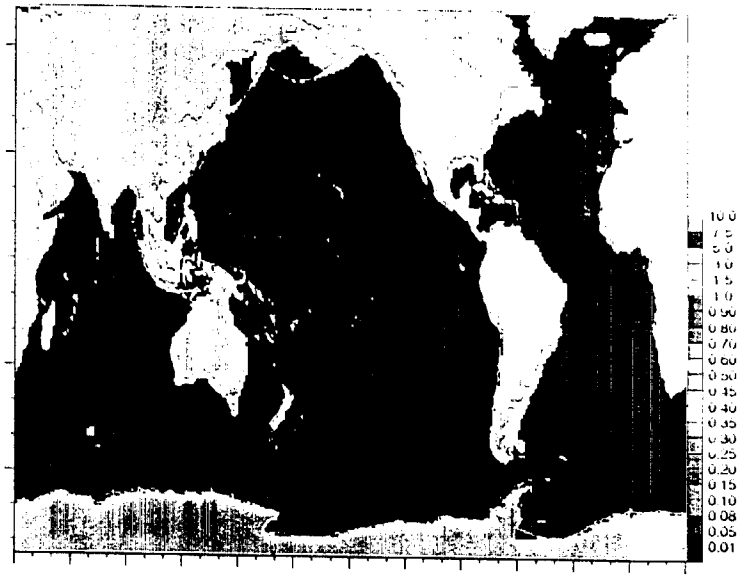

Cyanobacteria

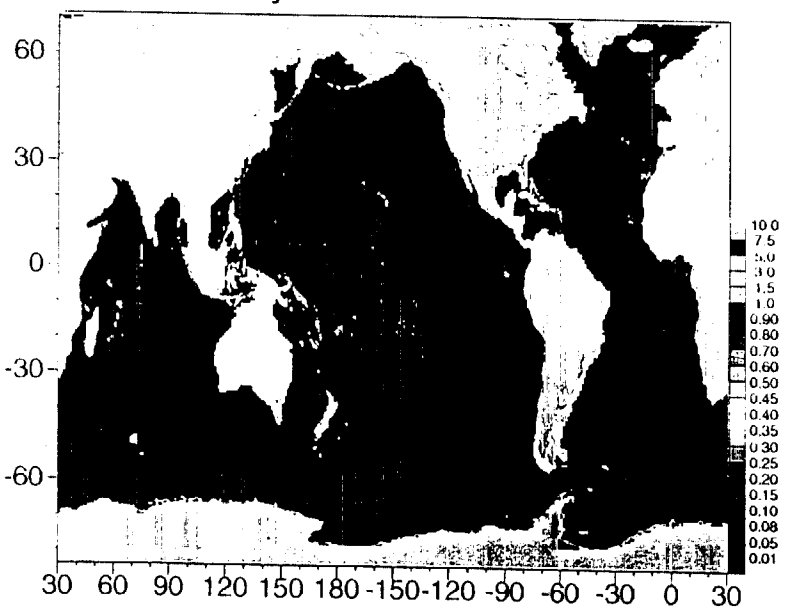

Coccolithophores

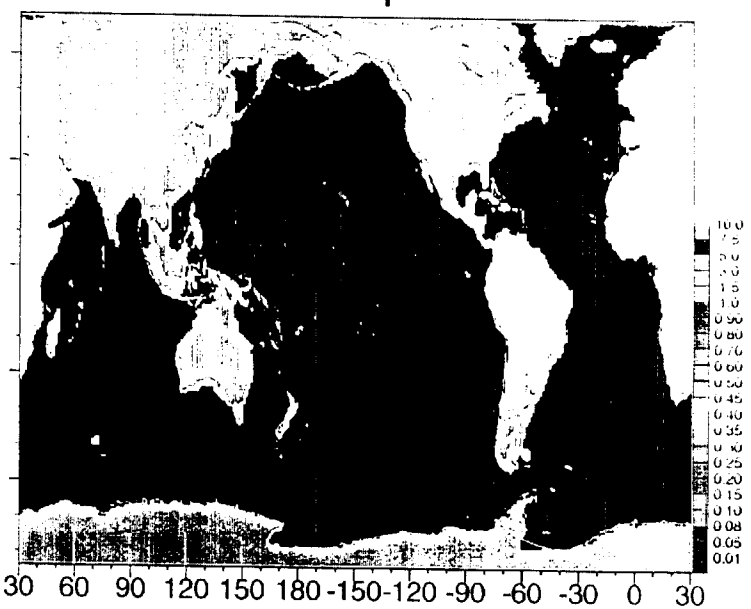

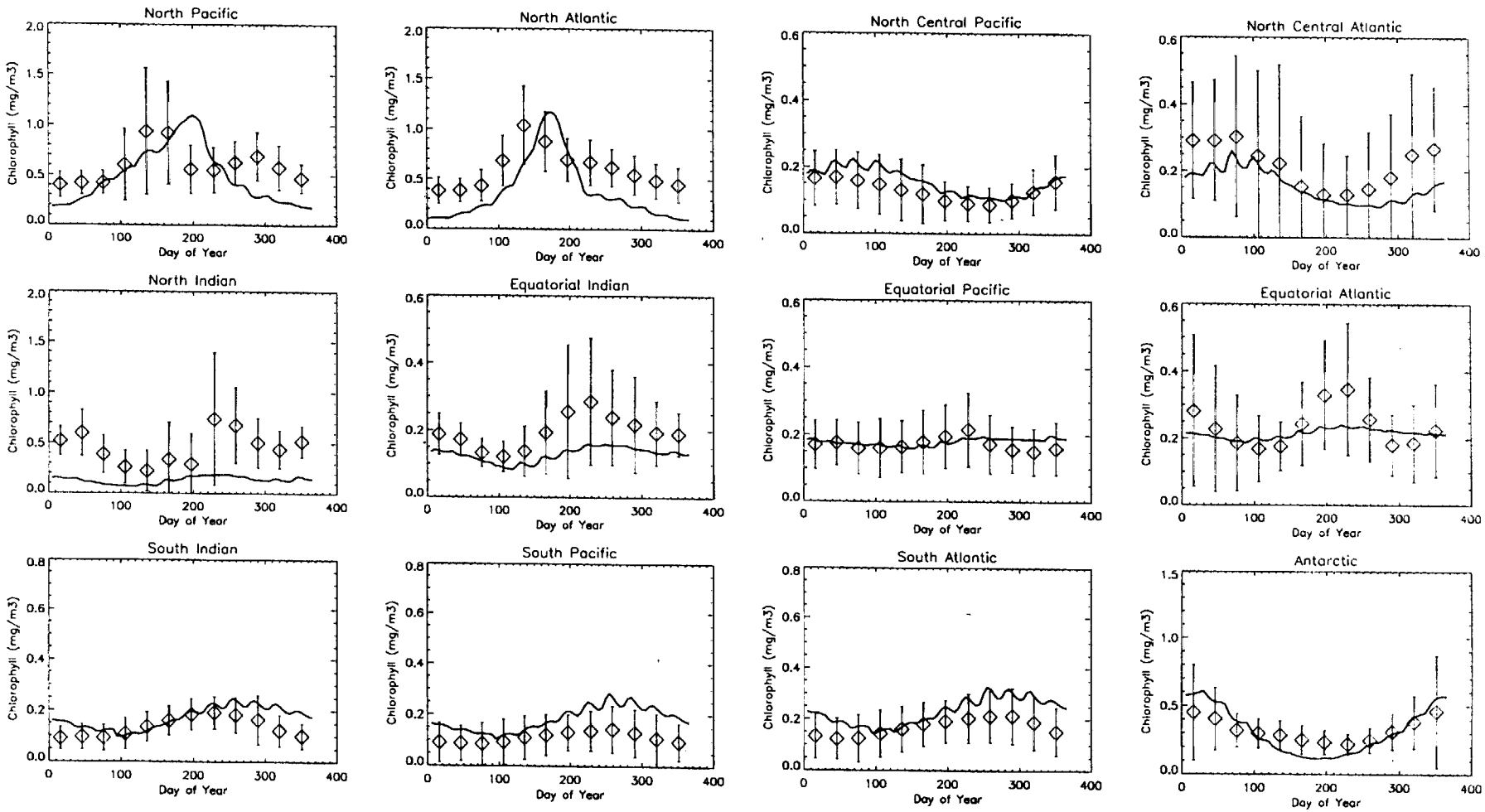
North Pacific
North Atlantic
North Central Pacific
North Central Atlantic
North Indian
Equatorial Indian
Equatorial Pacific
Equatorial Atlantic
South Indian
South Pacific
South Atlantic
Antarctic
Chlorophyll (mg/m3)
Day of Year

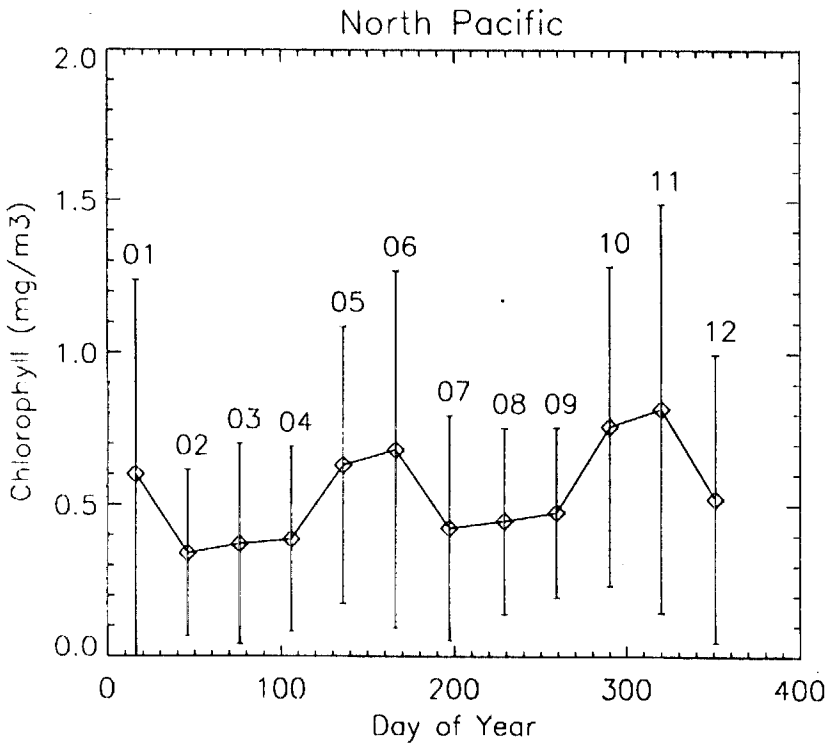
North Pacific
Chlorophyll (mg/m3)
2.0
1.5
1.0
0.5
0.0
0
100
200
300
400
Day of Year
01
02
03
04
05
06
07
08
09
10
11
12

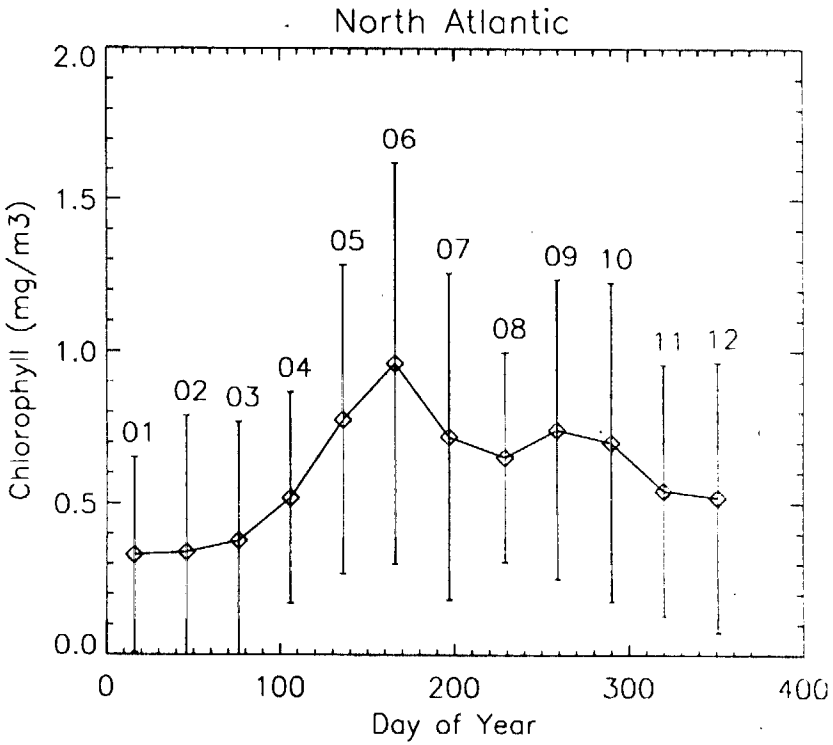
North Atlantic
Chlorophyll (mg/m3)
2.0
1.5
1.0
0.5
0.0
0
100
200
300
400
Day of Year
01
02
03
04
05
06
07
08
09
10
11
12

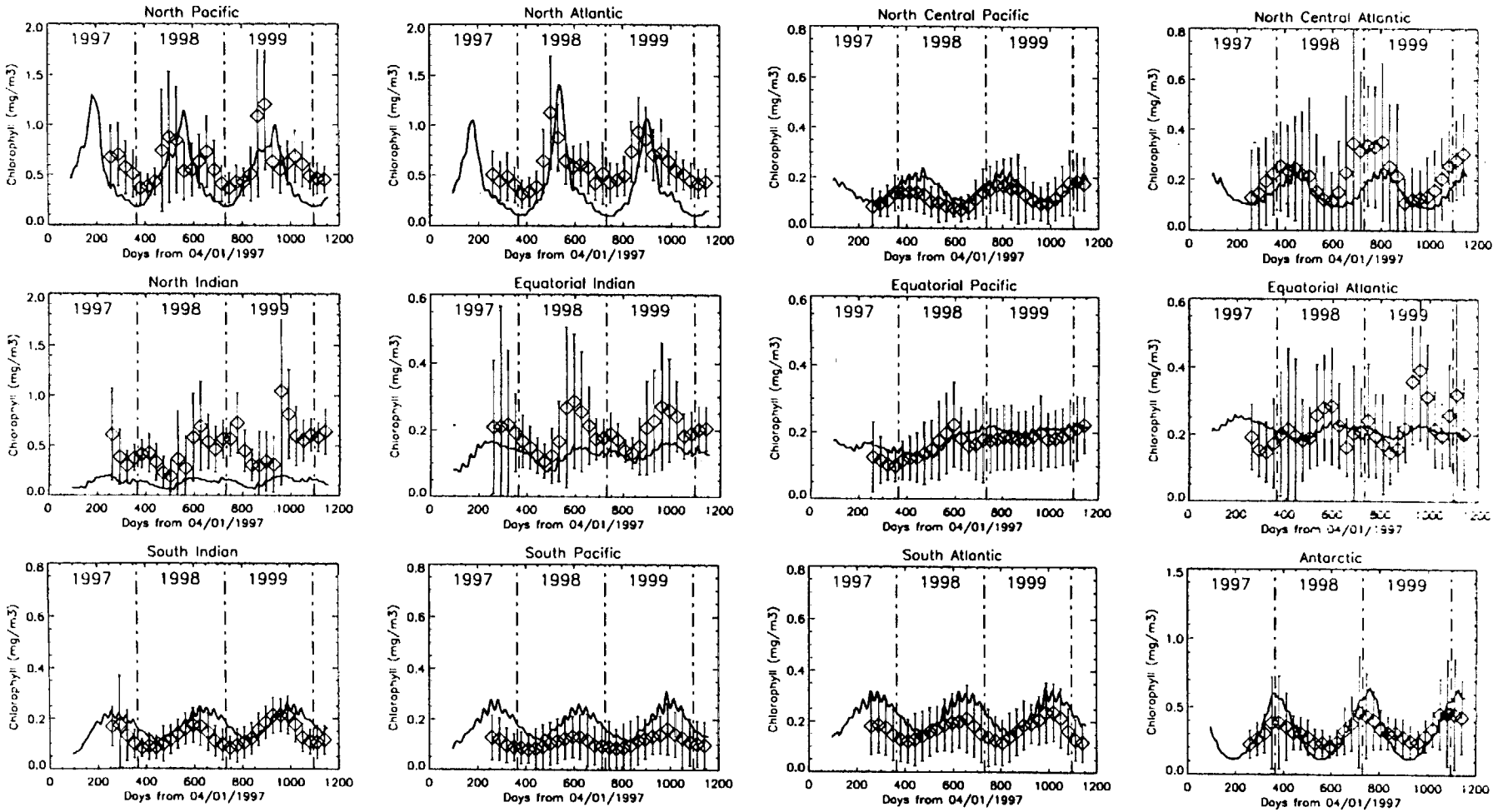
North Pacific
North Atlantic
North Central Pacific
North Central Atlantic
North Indian
Equatorial Indian
Equatorial Pacific
Equatorial Atlantic
South Indian
South Pacific
South Atlantic
Antarctic
1997
1998
1999
Chlorophyll (mg/m3)
Days from 04/01/1997

Model Chlorophyll ; November 1997

SeaWiFS Chlorophyll; November 1997

Model Chlorophyll ; February 1998

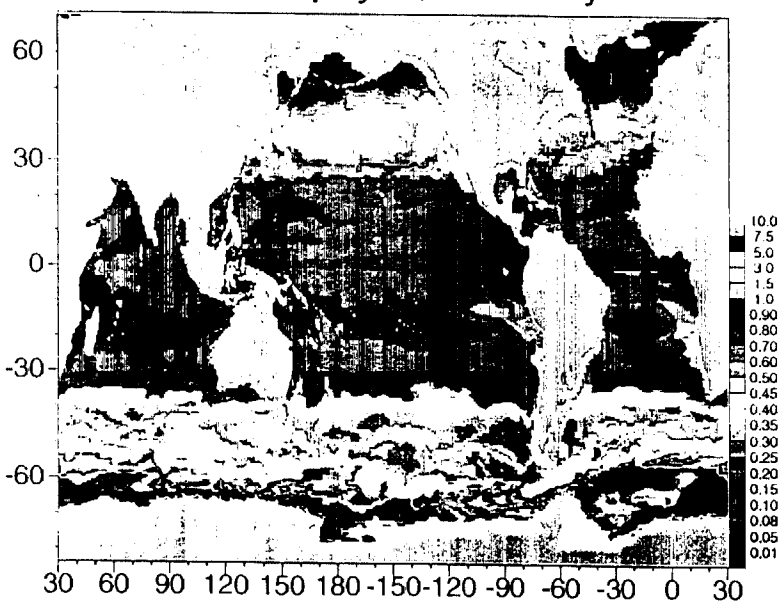

SeaWiFS Chlorophyll; February 1998

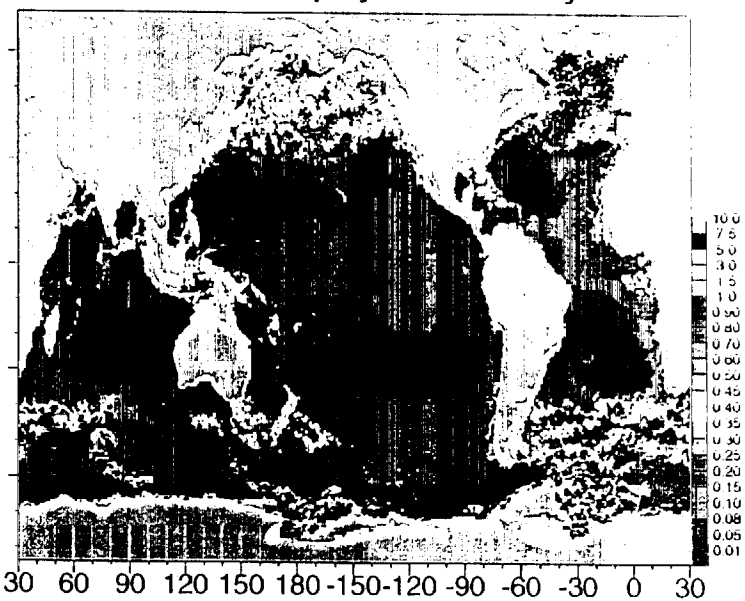

Model Chlorophyll ; August 1998

SeaWiFS Chlorophyll; August 1998

Model Chlorophyll ; March 1999

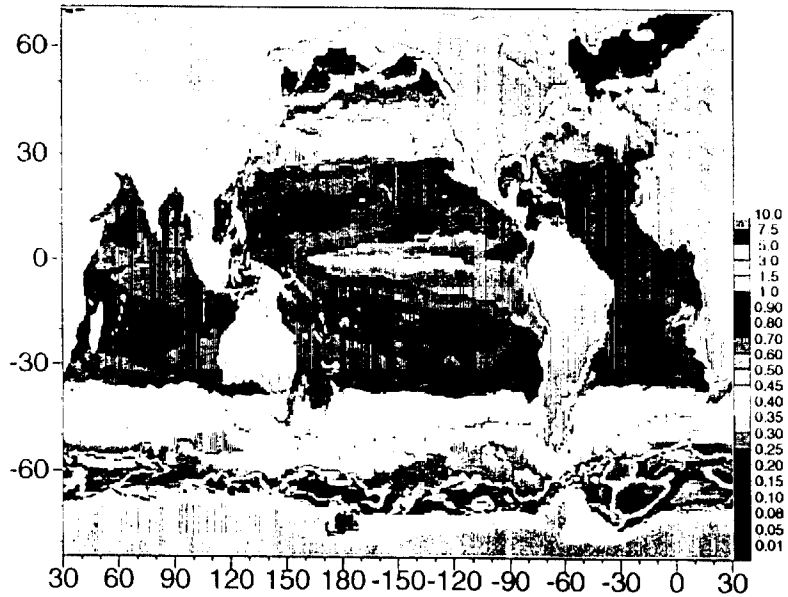

SeaWiFS Chlorophyll; March 1999

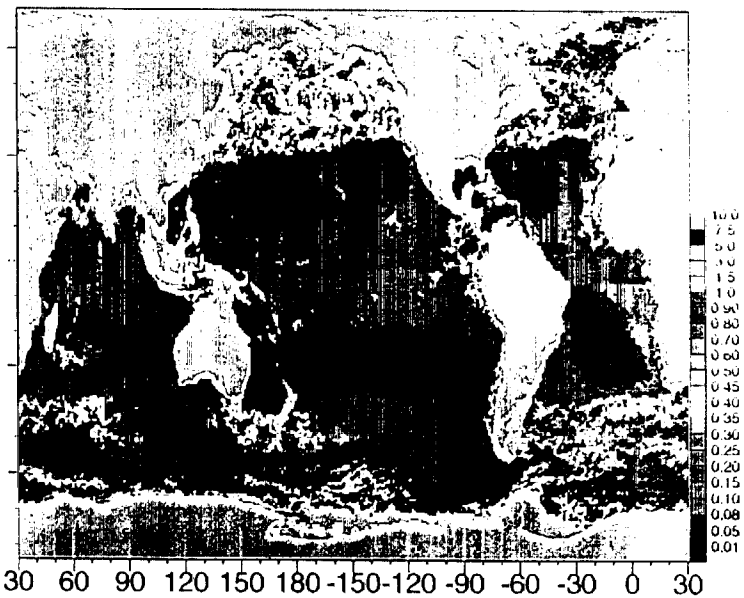

Nitrate Nov 1997

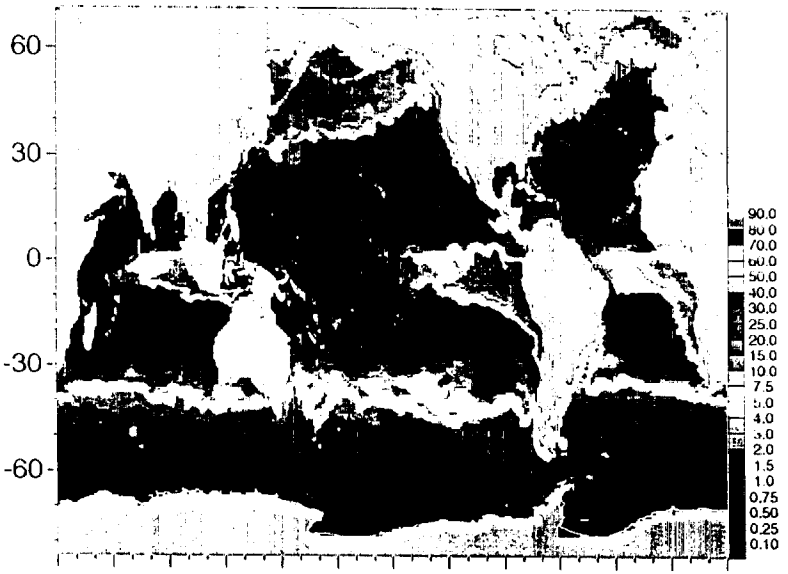

Nitrate May 1998

Nitrate Jun 1998

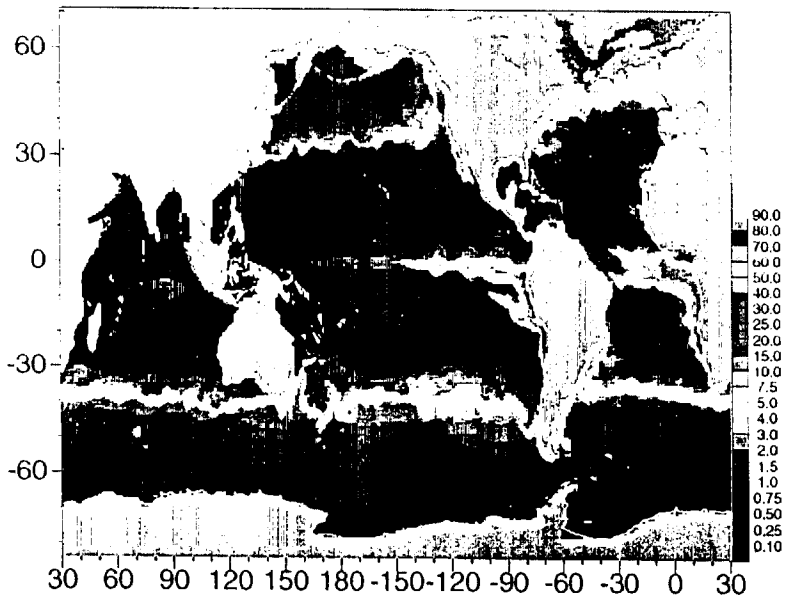

Nitrate Sep 1999

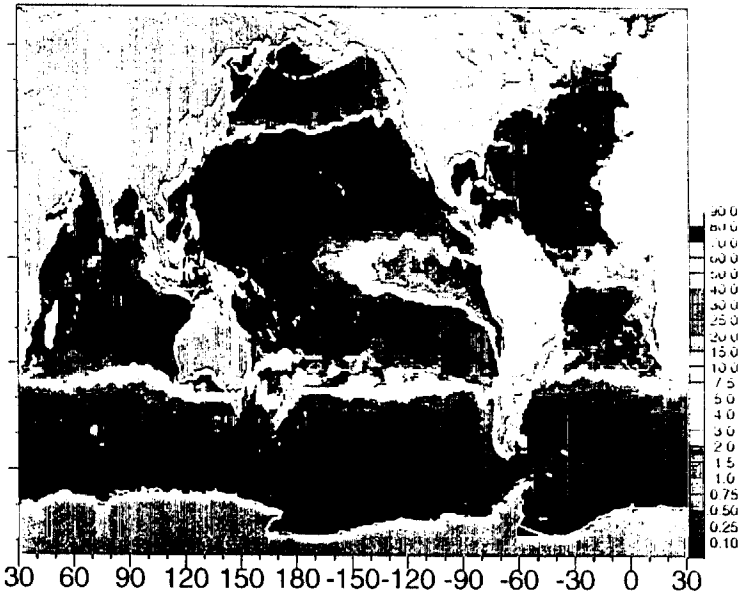

Model Chlorophyll ; July 1999

SeaWiFS Chlorophyll; July 1999

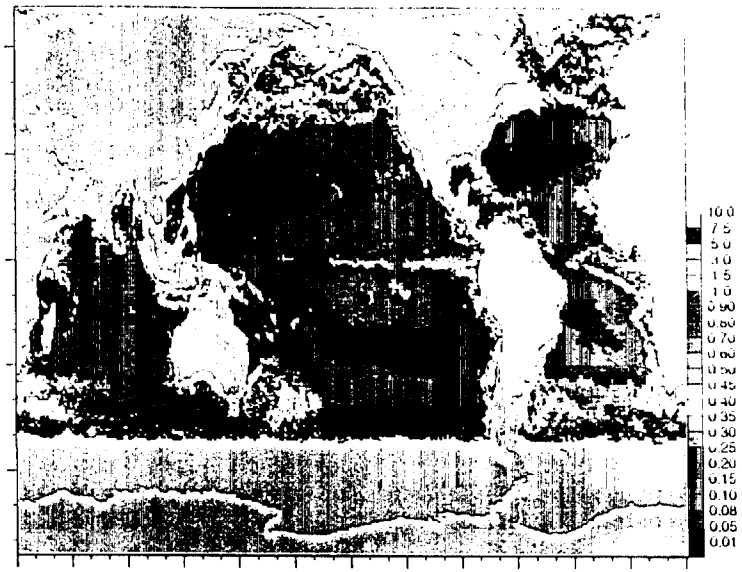

Model Chlorophyll ; February 2000

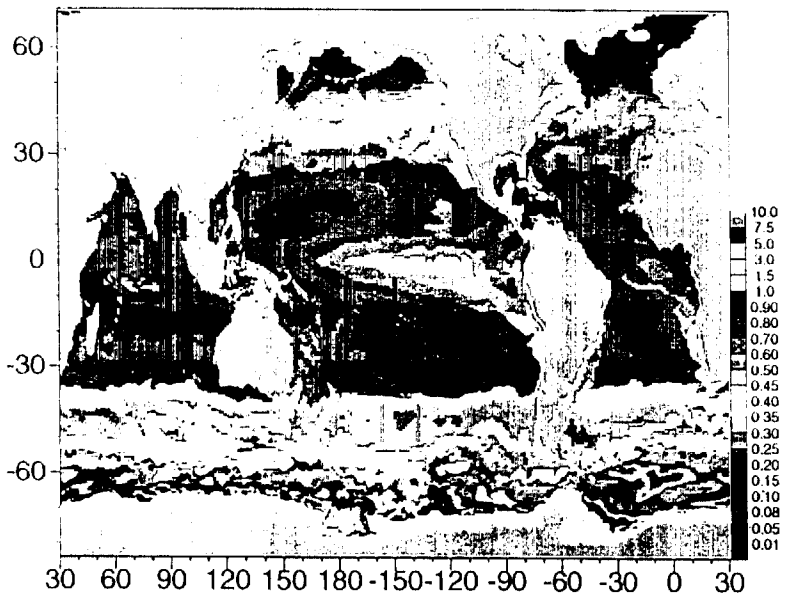

SeaWiFS Chlorophyll; February 2000

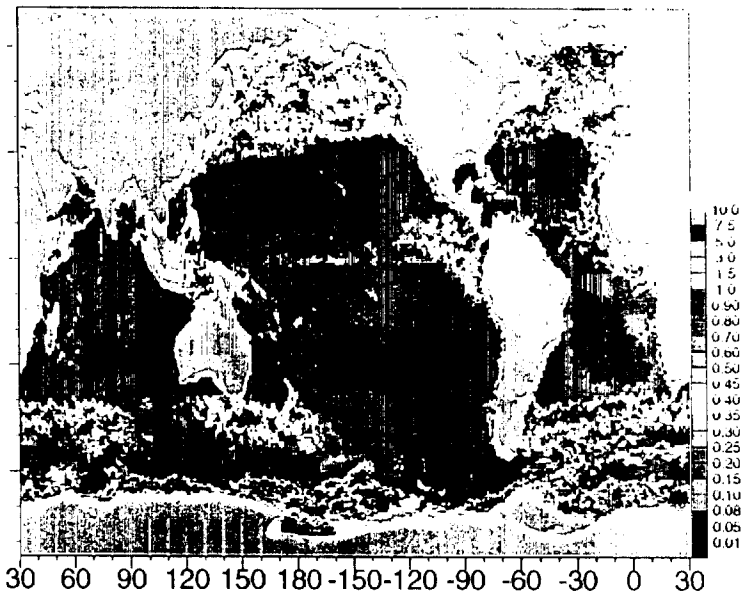

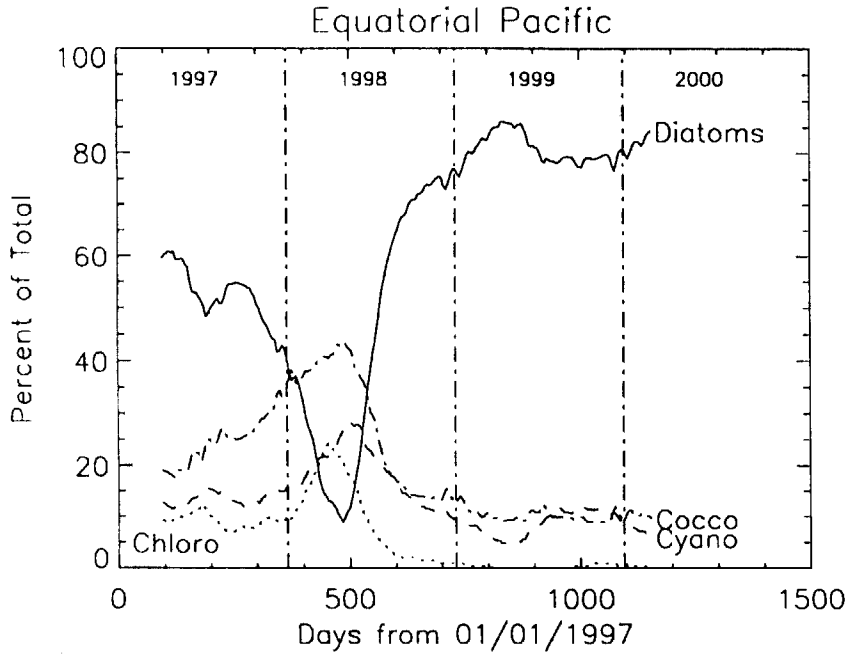
Equatorial Pacific
1997
1998
1999
2000
Diatoms
Cocco
Cyano
Chloro
Percent of Total
Days from 01/01/1997
0
20
40
60
80
100
0
500
1000
1500

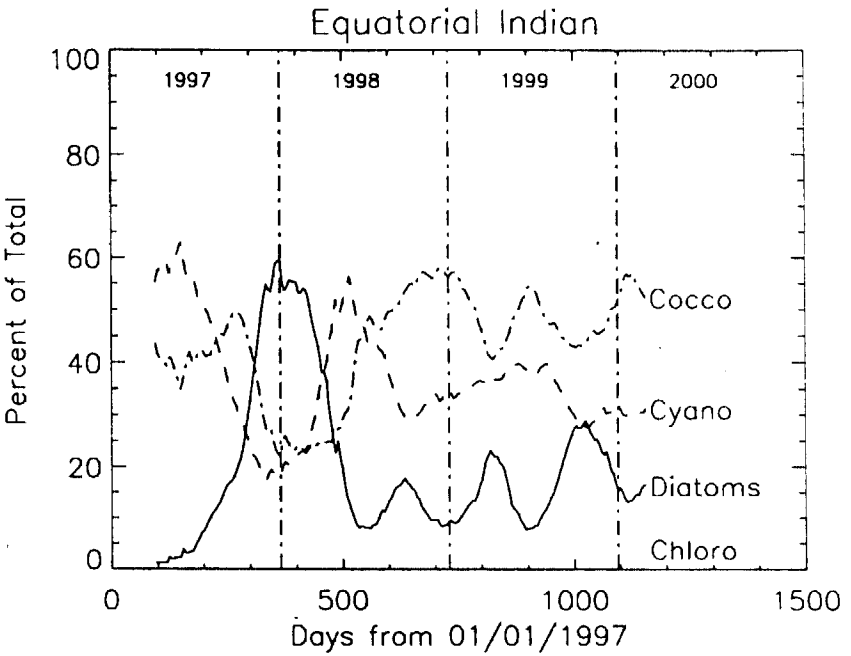
Equatorial Indian
1997
1998
1999
2000
Cocco
Cyano
Diatoms
Chloro
Percent of Total
Days from 01/01/1997
0
20
40
60
80
100
0
500
1000
1500

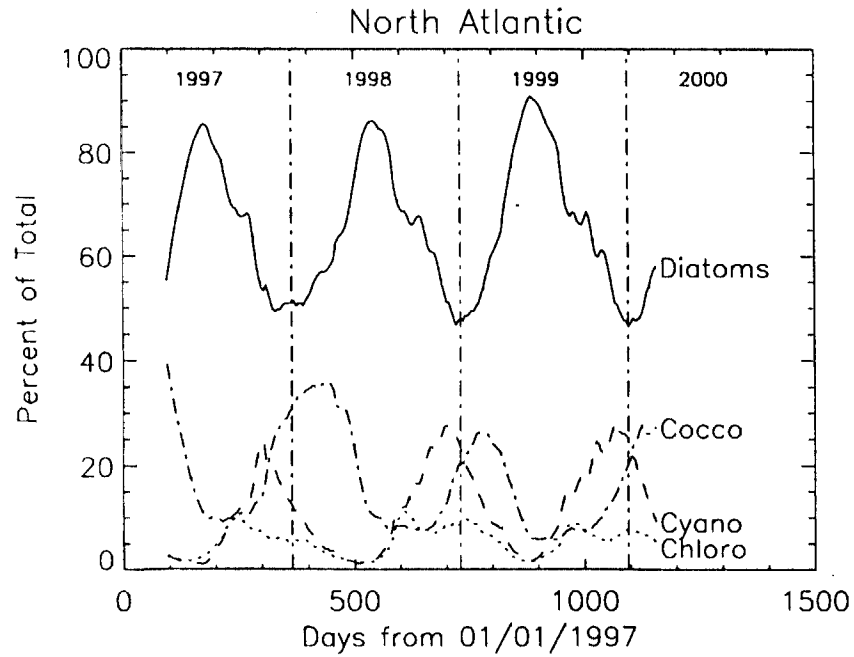
North Atlantic
1997
1998
1999
2000
Diatoms
Cocco
Cyano
Chloro
Percent of Total
Days from 01/01/1997
0
20
40
60
80
100
0
500
1000
1500

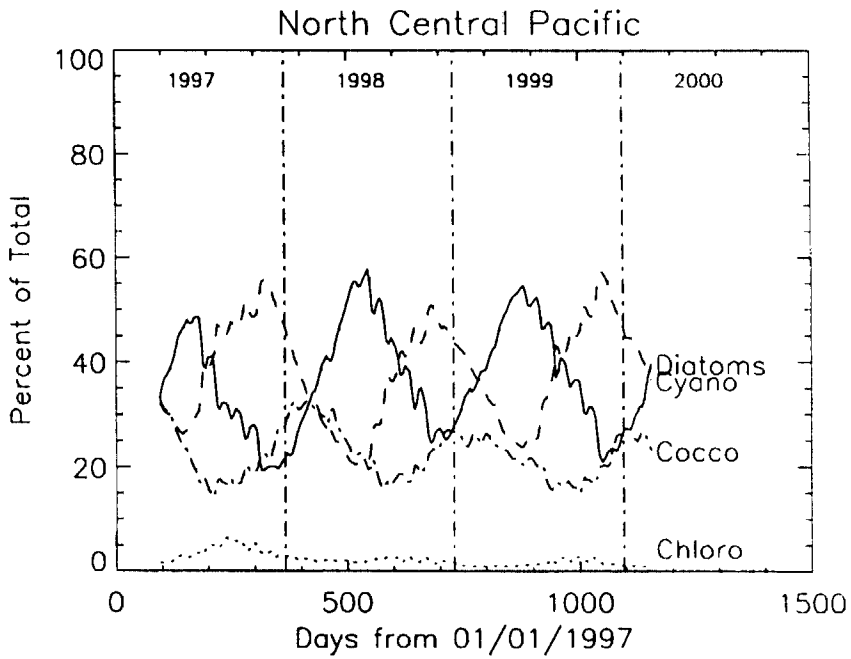
North Central Pacific
1997
1998
1999
2000
Diatoms
Cyano
Cocco
Chloro
Percent of Total
Days from 01/01/1997
0
20
40
60
80
100
0
500
1000
1500